REPORT DOCUMENTATION PAGE

Form Approved OMB NO. 0704-0188

1. REPORT DATE (DD-MM-YYYY)	2. REPORT TYPE	3. DATES COVERED (From - To)
31-01-2013	Final Report	1-Nov-2010 - 31-Oct-2012

4. TITLE AND SUBTITLE

Mitochondrial Damage: A Diagnostic and Metabolic Approach in Traumatic Brain Injury and Post-Traumatic Disorder

5a. CONTRACT NUMBER

W911NF-11-1-0005

5b. GRANT NUMBER

5c. PROGRAM ELEMENT NUMBER

0D10BG

6. AUTHORS

Pushpa, Sharma, Ph.D:Grunberg, Neil, Ph.D:Li, He, Ph.D:Berry, Erin, MS:Benford, Brandi, MS

5d. PROJECT NUMBER

5e. TASK NUMBER

5f. WORK UNIT NUMBER

7. PERFORMING ORGANIZATION NAMES AND ADDRESSES

The Henry M. Jackson Foundation
Office of Sponsored Programs
1401 Rockville Pike, STE 600
Rockville, MD 20852 -

8. PERFORMING ORGANIZATION REPORT NUMBER

9. SPONSORING/MONITORING AGENCY NAME(S) AND ADDRESS(ES)

U.S. Army Research Office
P.O. Box 12211
Research Triangle Park, NC 27709-2211

10. SPONSOR/MONITOR'S ACRONYM(S)

ARO

11. SPONSOR/MONITOR'S REPORT NUMBER(S)

58364-MS-DRP.1

12. DISTRIBUTION AVAILIBILITY STATEMENT

Approved for Public Release; Distribution Unlimited

13. SUPPLEMENTARY NOTES

The views, opinions and/or findings contained in this report are those of the author(s) and should not contrued as an official Department of the Army position, policy or decision, unless so designated by other documentation.

14. ABSTRACT

Our specific aims are: a)determine if blood based dipstick test of mitochondrial damage can predict the severity of metabolic failure and brain injury after TBI or TBI with preexisting stress(PTSD+TBI), b)study pyruvate as a countermeasure to mitigate mitochondrial functions in injured brain. Male Sprague Dawley rats with TBI,PTSD and PTSD+TBI were treated with/out pyruvate. We found that even one week after TBI, the metabolic, neurobehavioral parameters and expression of cellular proteins were altered. Blood base dipstick test of PDH

15. SUBJECT TERMS

Traumatic Brain Injury,Post-Traumatic Stress Disorder, Mitochondria, Dipstick, PHD, Complex I, Pyruvate, Apoptosis, Rats

16. SECURITY CLASSIFICATION OF:			17. LIMITATION OF ABSTRACT	15. NUMBER OF PAGES	19a. NAME OF RESPONSIBLE PERSON
a. REPORT	b. ABSTRACT	c. THIS PAGE			Pushpa Sharma
UU	UU	UU	UU		19b. TELEPHONE NUMBER: 301-295-9642

Report Title

Mitochondrial Damage: A Diagnostic and Metabolic Approach in Traumatic Brain Injury and Post-Traumatic Disorder

ABSTRACT

Our specific aims are: a)determine if blood based dipstick test of mitochondrial damage can predict the severity of metabolic failure and brain injury after TBI or TBI with preexisting stress(PTSD+TBI), b)study pyruvate as a countermeasure to mitigate mitochondrial functions in injured brain. Male Sprague Dawley rats with TBI,PTSD and PTSD+TBI were treated with/out pyruvate. We found that even one week after TBI, the metabolic, neurobehavioral parameters and expression of cellular proteins were altered. Blood base dipstick test of PDH enzyme as a biomarker of mitochondrial damage showed a good correlation. Pyruvate treatment showed neuroprotective properties in spite of muscle damage.

Enter List of papers submitted or published that acknowledge ARO support from the start of the project to the date of this printing. List the papers, including journal references, in the following categories:

(a) Papers published in peer-reviewed journals (N/A for none)

Received	Paper

TOTAL:

Number of Papers published in peer-reviewed journals:

(b) Papers published in non-peer-reviewed journals (N/A for none)

Received	Paper

TOTAL:

Number of Papers published in non peer-reviewed journals:

(c) Presentations

Number of Presentations: 1.00

Non Peer-Reviewed Conference Proceeding publications (other than abstracts):

Received Paper

TOTAL:

Number of Non Peer-Reviewed Conference Proceeding publications (other than abstracts):

Peer-Reviewed Conference Proceeding publications (other than abstracts):

Received Paper

TOTAL:

Number of Peer-Reviewed Conference Proceeding publications (other than abstracts):

(d) Manuscripts

Received Paper

TOTAL:

Number of Manuscripts:

Books

Received Paper

TOTAL:

Patents Submitted

Patents Awarded

Awards

Graduate Students

NAME	PERCENT_SUPPORTED
FTE Equivalent:	
Total Number:	

Names of Post Doctorates

NAME	PERCENT_SUPPORTED
FTE Equivalent:	
Total Number:	

Names of Faculty Supported

NAME	PERCENT_SUPPORTED
FTE Equivalent:	
Total Number:	

Names of Under Graduate students supported

NAME	PERCENT_SUPPORTED
FTE Equivalent:	
Total Number:	

Student Metrics

This section only applies to graduating undergraduates supported by this agreement in this reporting period

The number of undergraduates funded by this agreement who graduated during this period:	0.00
The number of undergraduates funded by this agreement who graduated during this period with a degree in science, mathematics, engineering, or technology fields:.....	0.00
The number of undergraduates funded by your agreement who graduated during this period and will continue to pursue a graduate or Ph.D. degree in science, mathematics, engineering, or technology fields:.....	0.00
Number of graduating undergraduates who achieved a 3.5 GPA to 4.0 (4.0 max scale):	0.00
Number of graduating undergraduates funded by a DoD funded Center of Excellence grant for Education, Research and Engineering:	0.00
The number of undergraduates funded by your agreement who graduated during this period and intend to work for the Department of Defense	0.00
The number of undergraduates funded by your agreement who graduated during this period and will receive scholarships or fellowships for further studies in science, mathematics, engineering or technology fields:	0.00

Names of Personnel receiving masters degrees

NAME

Total Number:

Names of personnel receiving PHDs

NAME

Total Number:

Names of other research staff

NAME PERCENT_SUPPORTED

FTE Equivalent:

Total Number:

Sub Contractors (DD882)

Inventions (DD882)

Scientific Progress

Technology Transfer

Mitochondrial Damage: A Diagnostic and Metabolic Approach in Traumatic Brain Injury and Post-Traumatic Disorder

Final Report- Cover Page

Date:	January 29, 2013
Grant Number:	58364-MS-DRP
Funding Agency:	Defense Advanced Research Projects Agency
Submitted to:	Dr. Geoff Ling (DARPA) Dr. David Stepp (ARO)
Principal Investigator:	Pushpa Sharma, Ph.D. Department of Anesthesiology Uniformed Services University of the Health Sciences Bethesda, MD 20814 Phone: 301-295-9642 Fax: 301-295-9642
E mail:	"Pushpa Sharma" <psharma@usuhs.edu>

Table of Contents

4. Introduction

It is becoming clear that traumatic brain injury (TBI) arising from blast exposure during Iraq and Afghanistan war is common, and frequently complicated by psychiatric morbidity related post-traumatic stress disorder (PTSD). Severe brain injuries can be identified and treated but mild traumatic brain injury (mTBI) is not well defined and many of its signs and symptoms often overlap with those of PTSD. [1-3] In a combat zone, it is possible that the very same event that causes a concussion or mild brain injury could also be life threatening, and often lead to PTSD in some while others may heal up completely within short time.[1-3] There may be a possibility of severe pre-existing stress due to war and/or fear of injury in some while in others it may not be the same case. In both cases (mTBI and PTSD), there are no outward signs of brain injury, but cells deep within the brain can be distorted due to their altered metabolism and mitochondrial pathways, causing them to die.[4, 5] We currently cannot see with routine computed tomography (CT scan) and Magnetic resonance imaging (MRI).[6, 7] Therefore, in battlefield and in remote areas, monitoring of mitochondrial damage and designing of therapeutic strategies in human head injury continues to remain a challenge for clinicians and researchers.

Most of the symptoms of mTBI and PTSD are the result of secondary cell injury cascade and metabolic failure due to the damaged mitochondria. Potent mitochondrial permeability inhibitor such cyclosporine A in the treatment of TBI, and anxiolytic and antidepressant agents, such as monoamine oxidase inhibitors (MAOIs) to improve mitochondrial efficiency and function against TBI and stress related disorders suggesting mitochondrial function may be linked to the pathophysiology and treatment of TBI, and behavioral/mood disorders. Furthermore, neuro-imaging studies of injured brain and depressed individuals show abnormalities in glucose metabolism and cerebral blood flow in various brain regions including the limbic and prefrontal cortex, the hippocampus and amygdala. Energetically active cells such as neurons require a more efficient ATP supply, which can only be provided by the glucose metabolism through the mitochondrial enzyme pyruvate dehydrogenase complex (PDH), and mitochondrial oxidative phosphorylation through its electron transport chain (ETC). The ETC is composed of five multi subunit enzyme complexes: NADH-ubiquinone reductase, (complex I), succinate-ubiquinone reductase, (complex II), ubiquinone-cytochrome c reductase (complex III), cytochrome c oxidase (complex IV) and ATP synthase (complex V).

Targeting mitochondrial functions may represent a novel avenue for the development of therapeutics for the treatment of stress-related disorders. The ineffective treatment of mild TBI and PTSD is mainly due to: **1)** a lack of sensitive biomarkers of mitochondrial damage to identify the similarities and differences between the metabolic failure in brain after TBI and PTSD and **2)** inadequate knowledge about the mitochondrial targeted metabolic therapies in the treatment of brain injury after TBI and PTSD. Providing metabolic support to the injured mitochondria by pyruvate- Glucose is an obligatory metabolic fuel for brain. Pyruvate is the end product of glucose metabolism, a natural allosteric activator of PDH enzyme, and can easily cross the blood brain barrier, improve neuronal energy via preventing mitochondrial damage, intracellular calcium buffering, reduced apoptosis and increased cognitive behavior.[8-12] Based on our recent findings[11], we ***hypothesize*** that a mitochondria- focused early diagnosis and treatment could increase the neuronal injury tolerance and alleviate the late consequences of TBI and PTSD. ***We also hypothesize*** that pre-exposure to the severity of stress and TBI will affect the outcome of developing PTSD symptoms.

5. Project Objectives:

The goals of this research proposal are to identify, develop, and possibly modify mitochondrial functions in injured brain by means of noninvasive dipstick test. Our **specific objectives** are: **a)** identify the appropriate set of novel dipstick based technologies along with their representative feature vectors of mitochondrial damage that can be used as early biomarkers to predict the severity of metabolic failure and brain injury after mild TBI or PTSD and **b)** develop mitochondrial targeted countermeasures to mitigate mitochondrial functions in injured brain.

Significance of the proposed research: At the completion of this research proposal, we expect to identify the mitochondrial, inflammatory and/or neurobehavioral biomarkers of TBI and PTSD. We may also determine if pyruvate can or can't be used for the treatment of TBI and PTSD.

6. Study design:

Sprague dawley rats weighing 250-300G were used in this study and placed in the in an environmentally controlled animal facility under a 12-h reverse light–dark cycle. Food and water were available ad libitum. Rats were left to acclimate for 1 week to the vivarium before use. All procedures were performed according to the National Institutes of Health (NIH) guidelines and were approved by the Institutional Animal Care and Use Committee (IACUC). Animals were divided into the following groups based on the type of treatment and its duration. All animals were subjected to a battery of neurobehavioral tests for the complete duration of the experiment.

Group 1. Naiive: These animals were time matched and did not receive any brain injury.

Group 2. TBI: Lateral fluid percussion injury was induced according to our published procedure, originally described by Dixon and modified by Ling et.al (2004).

Group 3. Naiive + pyruvate: These animals received sodium pyruvate (1g/kg) orally every 24 h for 7 days. Blood and brain ere collected as described in group 2.

Group 4. TBI+ pyruvate: Within 30 min after TBI, these animals received sodium pyruvate (1g/kg) orally every 24 h for 7 days. All animals were monitored for their neurobehavioral functions for 7 days post TBI.

Group 5. PTSDs: Short term(s) PTSD was induced by animal immobilization and induction of tail shock repeated for three consecutive days. Detailed procedure is described by Li et al.

Group 6. PTSDs+ TBI: This set of experiment was designed to examine the effect of pre-existing stress on the outcome of TBI. At 24 h post PTSD, animal received TBI by fluid percussion and monitored for 7 days post TBI at which time the experiment was terminated.

Group 7. PTSDs+ pyruvate: Within 30 min after stress procedure, sodium pyruvate (1g/kg) orally was given every 24 h for 7 days at which time the experiment was terminated.

Group 8. PTSDs+ TBI+pyruvate: Within 30 min after TBI, sodium pyruvate (1g/kg) orally was given every 24 h for 7 days at which time the experiment was terminated.

Group 9. PTSDL: PTSD with long term follow up. Animals in this group were followed for neurobehavioral functions for the next four weeks after exposure to the stress induced by their immobilization and induction of tail shock.

Group 10. PTSD+ TBI-L: Animals in this group received stress followed by TBI and monitored for neurobehavioral functions for next four weeks. Acute or short term PTSD was induced by immobilization animal and induction of tail shock repeated for three consecutive days.

7. Techniques:

a. Traumatic brain injury by fluid percussion: Traumatic brain injury was induced in rats using a fluid percussion injury (FPI) device (VCU Biomedical Engineering, Richmond, VA,USA). The procedure was initially described by McIntosh *et al*. and modified by Ling *et.al*. [15, 16] Animals were anesthetized with 1-3% isoflurane in oxygen. Under controlled physiological conditions and at 37°C, FPI was induced by performing a 3cm sagittal incision along the midline to expose the cranium. A 5mm burr hole was placed 2mm to the right of the sagittal suture halfway between bregma and lamda using a 5mm trephine drill bit exposing the dura. A Luer-Loc needle hub was placed into the burr hole and cemented to the cranium using cyanoacrilate. The glue was allowed to completely dry, and the empty Luer-Loc hub was filled with normal saline before being connected to the TBI device. A fluid percussion pulse of 2.5-3 atm was administered by an injury cannula positioned parasagittally over the right cerebral cortex. The fluid percussion pulse was administered by a pendulum modulated fluid percussion biomechanical device (Richmond, VA), the Luer-Loc hub was removed and defects in the cranium was repaired with bone wax. The skin flap was stapled with a surgical skin stapler. Animal was allowed to stabilize in the warm blanket and was returned to animal facility (LAM) at our Uniformed Services University of the Health Sciences for further treatment and recovery till completion of the protocol.

b. PTSD rat model have been developed in which different stress paradigms provoke a wide range of behavioral responses. Intensely stressful experiences, aversive challenges, and situational reminders of a traumatic stress in PTSD animal models have resulted in long-term effects on behavioral, autonomic, and hormonal responses that mimic many of the clinical symptoms seen in patients with PTSD. The methodologies used to produce PTSD animal models include electric shock, social confrontations, stress-re-stress or time-dependent sensitization, underwater trauma, exposure of a rat to a predator, and the inescapable tail-shock model of traumatic stress. To establish a rat model of PTSD using highly stringent criteria we have

successfully developed and tested the inescapable tail-shock model of stress in rats and verified that short and long-lasting behavioral, biochemical and physiological alterations result (Manion et al., 2007a). [20] Importantly, the stress-induced behavioral and neurobiological symptoms in the rat models are very similar to those seen in PTSD patients. [20]

Animal Preparation and Stress Protocol: In our animal model, stress exposure consisted of a two-hour per day session of immobilization and tail-shocks, for three consecutive days. The animals were restrained in a Plexiglass tube, and 40 electric shocks (2 mA, 3 s duration) were applied at varying intervals (140 to 180 s) over the course of two hours on three consecutive days. This stress protocol was adapted from the "learned helplessness" paradigm in which animals undergo an aversive experience under conditions in which they cannot perform any adaptive response.[21] We stress the rats for three consecutive days because it has been previously demonstrated that repeated immobilization and tail-shock stress sessions for three days is more effective than a single stress session in producing physiological and behavioral abnormalities, such as elevations in basal plasma corticosterone levels, exaggerated acoustic startle

c. Collection of blood and brain tissue: The experiment was terminated by anesthetizing the animal with Isoflurane, and removing blood from the heart (rt. ventricle). The blood was collected for dipstick test, blood chemistry and cytokine profiling. The brain was also dissected and stored in liquid nitrogen for further use. Three animals from this group were also infused with formalin and the brains were used for immunohistochemistry.

d. Analysis of blood: With the help of a handheld I-STAT machine and our USUHS biochemical facility, markers of oxygen metabolism acid base index and several systemic circulatory metabolites such as glucose, lactate, were measured in blood at 7 days after TBI, PTSD or TBI+PTSD in animals with or without pyruvate treatment. Control (Naïve) animals did not receive any injury.

e. Pyruvate dehydrogenase and mitochondrial electron transport chain enzyme complex I were measured in blood and hippocampus by the use of dipstick test according to our published method.

f. Expression of mitochondrial targeted genes in TBI- A gene expression database was constructed using FileMaker software (FileMaker Pro, Inc., CA). Database construction, data filtering and selection were performed as described previously[13] [14].

g. Neurobehavioral analysis: All animals were subjected to NSSR and tests of memorry and cognetive functions.

h. High-throughput expression profiling of Cytokines in Serum, CSF and peri-lesional Brain tissue. To determine the validity of changes in expression profiles of Cytokines and other inflammatory markers in Serum, CSF and Specific Brain areas (Cortex and Hippocampus) with or without injury/PTSD, using antibody based microarray.

i. **Histochemical studies on peri-lesional brain tissues**. To determine the cellular expression profile and extent of injury and effect of treatment on the peri-lesional brain tissue with and without injury and/or stress.

j. **Statistical Analysis:** All results are presented as Mean ± SE of number of experiments per group. Results were also subjected to statistical analysis using one way ANOVA followed by Benforreni test.

8. Results:

a. Serum biomarkers of oxygen and glucose metabolism in response to TBI and/or PTSD, and effect of pyruvate treatment

In comparison to the baseline, all animals gained significant weight at the time of sacrifice. As shown in table 1 and 2. In comparison to controls, serum glucose was reduced significantly by TBI and PTSD short term suggesting increased glucose metabolism to meet the cellular metabolic demands (injured brain). In contrast, glucose was increased in long term PTSD and in all pyruvate treated animals suggesting low metabolic demands due to healthy cells. Compared with controls, serum lactate was not significantly altered in TBI or PTSD animals. However pyruvate signifiantly increased the serum lactate which may be used as a metabolic fuel by the injured neurons.

As shown in table 1, the pCO_2 in TBI animals remained similar to controls but it significantly decreased by pyruvate treatment. pCO_2 reflects the exchange of this gas through the lungs to the outside air.

As depicted in table 2, in contrast to TBI, all PTSD animals had reduced pCO_2 in comparison to controls. Decreased pCO_2 is caused by hyperventilation, hypoxia and or anxiety, and these are common characteristic in animals as well as in patients with injury. pO_2 (Partial Pressure of Oxygen) reflects the amount of oxygen gas dissolved in the blood. It primarily measures the effectiveness of the lungs in pulling oxygen into the blood stream from the atmosphere. The lower pO_2 in our PTSD animals confirmed poor oxygen supply in response to stress. TBI had no effect and pyruvate significantly increased the oxygen consumption in comparison to all other groups.

Base Excess reflects the accumulation of metabolically produced acids, the body attempts to neutralize those acids to maintain a constant acid-base balance. More positive Values of Base Excess may indicate loss of buffer base and /or hemorrhage. A positive value of BE in our rats with TBI and short term PTSD, confirms the chemical acidosis in injured brain tissue. In contrast, BE was significantly improved in long term PTSD suggesting the progress of healing process in four weeks post stress.

Stress proteins in response to TBI and/or stress- Serum cortisol was not altered in any of the group examined. However, CPK (creatine phosphokinase) as a marker of cell injury was increased in al TBI and short term PTSD animals, but not in long term PTSD animals. These observations indicate the presence of injury in TBI as well as in short term PTSD due to electric shock in tail. Low CPK in long term PTSD or PTSD+TBI suggest the progression of healing process by the end of four weeks post injury.

Table 1

Effect of pyruvate treatment on Blood gases, Acid base parameters and metabolites following TBI

Parameters	Control (18)	Control+Pyr (8)	TBI (19)	TBI+Pyr (8)
Weight before TBI	319.5±20.5,	272.8±1.9 [a]	305.0±12.9	276.5±2.8
Weight at sacrifice	336.8±19.7	285.4±8.0 [a]	332.2±20.7	270.5±6.4[#]
Glucose mg/dL	271.5±12.5	293.2±30.2	260.9±10.0	289.0±20.0
Lac mmol/L	2.4±0.7	2.9±0.2	2.9±0.3	2.6±0.3
pH	7.06±0.06	7.25±0.16	7.11±0.07	7.38±0.18 [#]
PCO_2 mmHg	64.8±6.0	29.6±3.4 [a]	55.6±5.0	35.2±4.4 [##]
PO_2 mmHg	82.3±10.7	77.3±16.8	74.0±10.3	118.1±29.2 [#]
HCO_3 mmol/L	26.7±1.0	20.9±1.1 [a]	26.1±0.7	21.8±0.8 [#]
BE mEq/L	−0.56±0.9	−2.88±1.3 [a]	−0.32±0.4	−2.5±1.0
SO_2%	82.4±4.4	91±7.0	78.7±5.1	89.3±5.1
CPK U/L	758.1±62.5	2535.0±929	1872.9±647	2917.6±540
Cholesterol mg/dL	257.3±47.2	532.8±168.2	180.8±35.9	536.1±168.2
Cortisol ug/dL	4.0±0.1	3.0±0.2	3.3±0.5	3.2±0.2
BUN mg	23.3±1.4	24.7±3.0	21.0±0.9	22.0±1.7
Na-mmol/L	134.7±0.4	140.3±3.0	134.8±0.8	140.1±2.7
K-mmol/L	7.12±0.5	15.85±5.1	6.63±0.5	17.50±5.8
Cl-mmol/L	101.6±1.37	100.5±2.2	101.2±1.4	99.9±1.7
AST U/L	79.7±2.5	109.3±10.0	83.3±2.0	146.4±13.4
ALT U/L	60.4±3.5	56.3±3.8	61.9±4.3	65.4±3.9

The data presented in are Mean ± SE of n number of animals in each group.

- $p<0.05$ Control vs. TB, [a] $p<0.05$, Control vs Control+Pyruvate, [#] $p<0.05$ TBI vs. TBI+Pyruvate

Table 2.

Effects of TBI with pre- existing acute or chronic stress on blood chemistry

Parameters	PTSDs (12)	PTSDs+Py (4)	PTSDs+TBI (10)	PTSDs+TBI +Py(4)	PTSD L(15)	PTSD+TBI L(8)
Weight before TBI	225.8±2.3	247.3±8.6	221.7±2.6	244.3±3.8	190.5±9.6	226.5±3.8
Weight at sacrifice	252.6±2.0	265±15.2	245.7±2.0[#]	260.5	322.5±7.1 [a]	332±6.7
Glucose mg/dL	N/A	240±22.8	243.8	252.5±21.3	267.9±17.2	259.1±9.5
Lac mmol/L	2.33±0.28	3.67±0.67	2.60±0.22	2.0±0.6	2.73±0.21	1.88±0.64
TCO_2 mmol/L	N/A	N/A	N/A	N/A	N/A	N/A
pH	7.0±0.01	7.0±0.01	7.2±0.13	7.0±0.01	7.19±0.04	7.10±0.01
PCO_2 mmHg	43.3±3.1	48.8±3.6	37.4±3.6[#]	44.8±5.8	75.5±5.0 [a]	88.0±3.9
PO_2 mmHg	53.0±9.1	48.0±11.0	70.0±16.9	70.0±15.7	56.9±10.7	53.5±9.6
HCO_3 mmol/L	24.3±1.0	25.5±1.0	23.3±1.0[#]	25.3±1.8	31.2±1.0[a]	33.0±0.9
BE mEq/L	−1.08±0.9	−0.5±0.7	−1.10±0.6[#]	0.25±1.3	3.93±0.8[a]	4.63±1.1

SO_2%	73.8±5.8	73.5±7.1	78±6.1 [#]	87.8±5.8	59.7±8.6[a]	66.0±9.4
CPK U/L	607±588	288±17.2	3123±123[#]	261±1.9	2223.5±1.9	324.8±39.6
Cholesterol mg/dL	127.6±267	94.0±4.7	966.8±240[#]	106.8±4.5	91.5±3.9[a]	78.4±2.1
Cortisol ug/dL	3.58±0.4	2.98±0.4	3.40±0.3	3.33±0.2	3.55±0.5	3.33±0.4
BUN mg	N/A	23±2.4	N/A	20±1.4	20.6±0.7	19.1±1.4
Na-mmol/L	N/A	140.8±0.9	N/A	141±0.6	140±1.7	130.6±5.0
K-mmol/L	N/A	5.0±0.1	N/A	4.5±0.3	5.5±0.4	7.8±2.9
Cl-mmol/L	N/A	99.7±0.5	N/A	100.5±0.5	98.6±1.0	90.9±3.1
AST U/L	N/A	85.5±3.9	N/A	81±2.1	8.1.8±3.3	89.8±5.7
ALT U/L	N/A	59.8±8.8	N/A	54.8±2.4	55.6±3.2	53.8±1.3

The data presented in are Mean ± SE of n number of animals in each group.

- p<0.05 PTSDS vs PTSDs+ TBI, [a] p<0.05 PTSDs vs PTSDL,
  [#]: PTSDs+ TBI vs PTSDs+ TBI+ Pyruvate

b. Measurement of Mitochondrial complex I and PDH enzyme content in whole blood by Dipstick test to determine the validity of this blood based dipstick test as a biomarker of the severity of head injury in TBI and/or PTSD.

Theory: Damaged mitochondria in injured brain generate maximum free radicals, which are released into the blood stream and can damage the mitochondria in PBMC of blood. Dipstick test is a very simple test and can be performed in 50-100 ul blood (depend on the severity of mitochondrial damage).

The data of dipstick test in blood for complex I and PDH is shown in Fig.1. The enzyme contents of complex I and PDH were significantly higher in the blood of TBI rats when compared with the control group, suggesting the adaptive mitochondrial response and repair process by 7day post TBI. Similar results were seen in blood from animals with short term PTSD (fig.2). However, in TBI, both complex I and PDH increased at the same rate, while in all PTSD's increase in complex I was lower than PDH suggesting the altered redox status or low substrate availability for complex I.The reason is that pyruvate treatment of PTSD significantly increased complex. In contrast, pyruvate treatment in TBI did not affect either complex I or

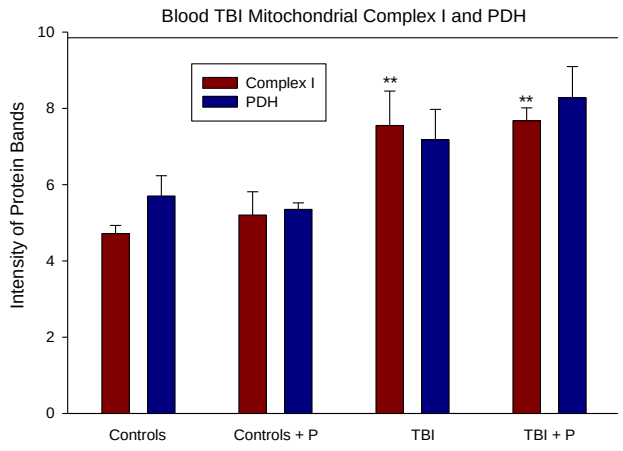

Fig,1. Results are M ± SE of protein intensity of bands from complex I and PDH in blood of TBI and TBI+py animals collected at d7. **<0.01 compared with controls. Dipstick test

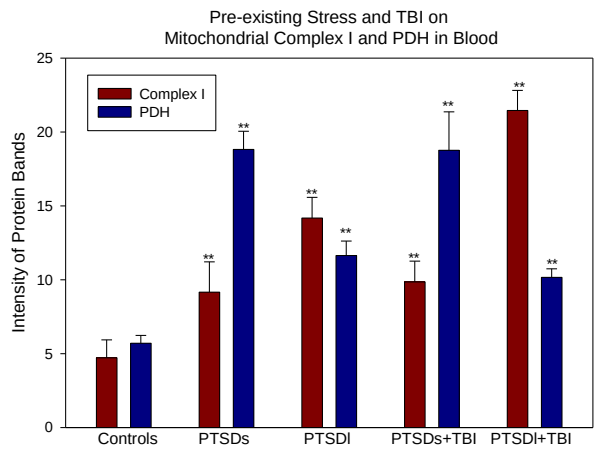

Fig.2. Results are M ± SE of protein intensity of bands from complex I and PDH in blood of PTSDs and PTSDs+py or PTSD long term animals collected at d7 or at 4 wks post TBI. **<0.01 compared with controls. Dipstick test

PDH. In short term PTSD blood samples, PDH content increased at a higher rate than complex I. Long term PTSD had similar increase in both enzymes. Also PDH increased in short term PTSD but not in long term PTSD

c. Measurement of Mitochondrial complex I and PDH enzyme content in hippocampus by Dipstick test

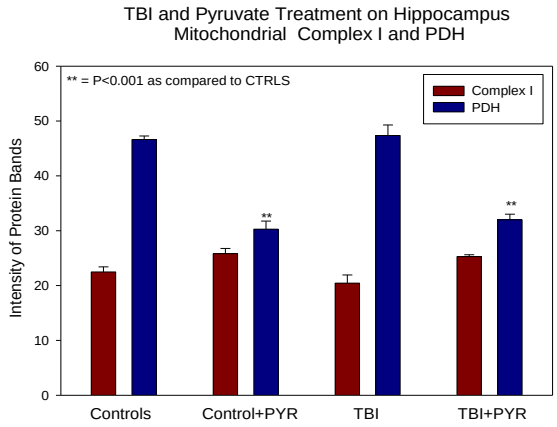

Fig.3. Results are M ± SE of protein intensity of bands from complex I and PDH in hippocampus of TBI and TBI+py animals collected at d7. **<0.01 compared with controls. Dipstick test

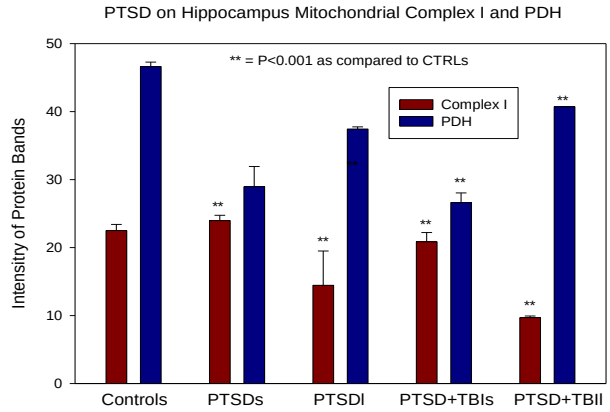

Fig.4. Results are M ± SE of protein intensity of bands from complex I and PDH in blood of PTSDs and PTSDs+py or PTSD long term animals collected at d7 or at 4 wks post TBI. **<0.01 compared with controls. Dipstick test

As shown in fig.3, not complex I but PDH was increased at day 7 post TBI suggesting increased substrate metabolism to meet the ATP demand of injured brain. The same observations were also seen in all PTSD animals. However, low complex I in long term PTSD suggest increase free radical content and thus damage to the electron transport chain. These changes in mitochondrial integrity may lead to secondary cell injury.

d. Correlation of PDH enzyme in blood vs. hippocampus

As shown in fig.5, and 6, there was a direct correlation between PDH contents in blood and hippocampus of animals with TBI or PTSD. Although these measurements are done in duplicate samples from three animals per gp, but the data is encouraging in showing the biomarkers of brain mitochondrial health in blood.

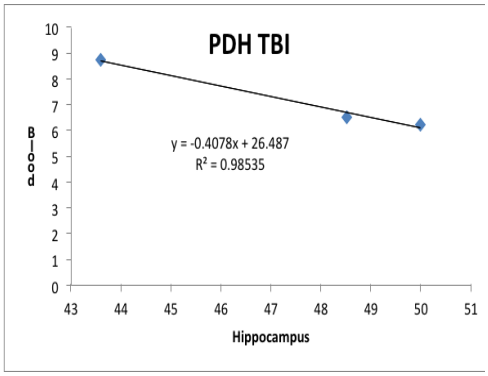

Fig.5.Correlation by linear regression in PDH contents in blood and hippocampus by dipstick test

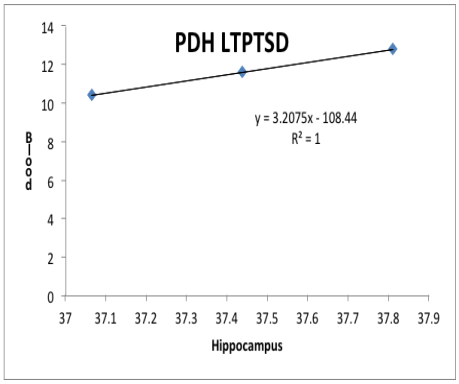

Fig.6. Correlation by linear regression in PDH contents in blood and hippocampus by dipstick test

e. Correlation of Complex I content in blood and hippocampus

There was a significant correlation between complex I in blood and hippocampus of only long term PTSD group. This corrrelation was not obserbed in any other gp.

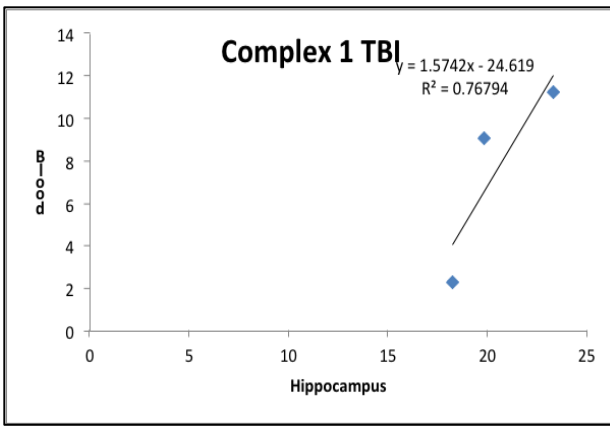

Fig.7. Correlation by linear regression in complex I contents in blood and hippocampus by dipstick test.

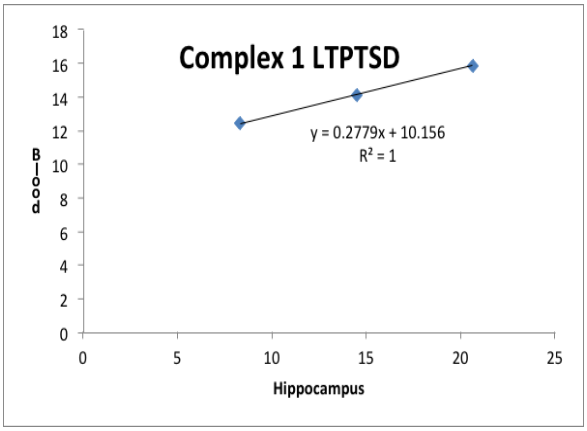

Fig.8. Correlation by linear regression in complex I contents in blood and hippocampus by dipstick test

f. Mitochondrial targeted Genetic profiling of TBI in hippocampus

Bioinformatics and systems biology analyses of the data depicted in table 3 showed 31 dysregulated genes, 10 affected canonical molecular pathways including a number of genes involved in mitochondrial enzymes for oxidative phosphorylation, mitogen-activated protein Kinase (MAP), peroxisome proliferator-activated protein (PPAP), apoptosis signaling, and genes responsible for long-term potentiation of Alzheimer's and Parkinson's diseases. Our results suggest that dysregulated mitochondrial-focused genes in injured brains may have a clinical utility for the development of future therapeutic strategies aimed at the treatment of TBI.

Table 3. Pathways with a Significant Number of Mitochondrial Dysregulated Genes in Rat TBI Hippocampus

KEGG_PATHWAY	Genes	Count	%	P-Value	Benjamini
Alzheimer's disease	Ndufs2, Atp5o, Fas, Cox5b, Apaf1, Chp	6	17.1	1.30E-03	7.90E-02
MAPK signaling pathway	Mapk12, Fas, Prkcg, Chp, Atf4, Ntrk1	6	17.1	4.70E-03	9.80E-02
Parkinson's disease	Ndufs2, Atp5o, Htra2, Cox5b, Apaf1	5	14.3	2.90E-03	8.90E-02
Apoptosis	Fas, Apaf1, Chp, Ntrk1	4	11.4	5.50E-03	8.50E-02
Oxidative phosphorylation	Atp6v0a1, Ndufs2, Atp5o, Cox5b	4	11.4	2.00E-02	2.30E-01
Huntington's disease	Ndufs2, Atp5o, Cox5b, Apaf1	4	11.4	4.60E-02	2.70E-01
Amyotrophic lateral sclerosis	Mapk12, Apaf1, Chp	3	8.6	2.60E-02	2.50E-01
Long-term potentiation	Prkcg, Chp, Atf4	3	8.6	3.30E-02	2.70E-01
PPAR signaling pathway	Fabp3, Cpt1b, Scp2	3	8.6	3.70E-02	2.60E-01
VEGF signaling pathway	Mapk12, Prkcg, Chp	3	8.6	4.00E-02	2.50E-01

g. Neurobehavioral Analyses in response to TBI, PTSD and pyruvate treatment

Naïve, TBI

- TBI caused more depression-related behaviors (vertical activity)
- TBI deleteriously affected neurobehavioral functioning (NSS-R)
- TBI deleteriously affected balance (rotarod)
- TBI decreased the startle response (ASR – all cases)

Naïve, TBI, Pyruvate

- TBI decreased activity (total distance and horizontal)
- TBI caused more depression-related behaviors (vertical activity)
- TBI deleteriously affected neurobehavioral functioning (NSS-R)
- TBI deleteriously affected balance (rotarod)
- TBI decreased the startle response (ASR – all cases)
- Pyruvate helped with balance (rotarod)
- Pyruvate decreased startle at T2 (ASR – all cases)

PTSD Short Term

- PTSD decreased activity (total distance, horizontal activity, movement time)
- PTSD caused more depression-related behaviors but TBI+PTSD had the most extreme effect (vertical activity)
- PTSD increased anxiety-related behaviors (center time)
- PTSD decreased grip strength at T2
- PTSD improved balance (rotarod)
- PTSD alone had no effect on startle (fairly consistent through all time points); TBI+PTSD showed an initial decrease in startle response and no improvement at T2 (ASR)
- TBI caused more depression-related behaviors (vertical activity)
- TBI deleteriously affected neurobehavioral functioning (NSS-R)
- TBI deleteriously affected balance (rotarod)
- TBI decreased the startle response (ASR – all cases)

PTSD Long Term

- The increases in activity at T2 may be due to the animals not remembering after a month (OFA)
- TBI deleteriously affected neurobehavioral functioning that persists (NSS-R)
- TBI deleteriously affected balance (rotarod); long term differences may be due to the animals not remembering after a month
- PTSD alone had no effect on startle (fairly consistent through all time points – even a month later); TBI+PTSD showed an initial decrease in startle response and an increase at T3 (ASR)

Long Term vs. Short Term PTSD

- There is an increase in activity (all OFA measures) in the long term animals, but this is most likely due to the animals not remembering after a month and they are re-exploring the chamber.

- TBI deleteriously affected neurobehavioral functioning that persists (NSS-R)
- TBI deleteriously affected balance (rotarod); long term differences may be due to the animals not remembering after a month.

PTSD alone had no effect on startle (fairly consistent through all time points – even a month later); both short and long term TBI+PTSD animals showed an initial decrease in startle response. Short term animals did not change at T2, but the long-term animals startle response increased slightly at T3 (but did not return to normal).

Open Field Activity

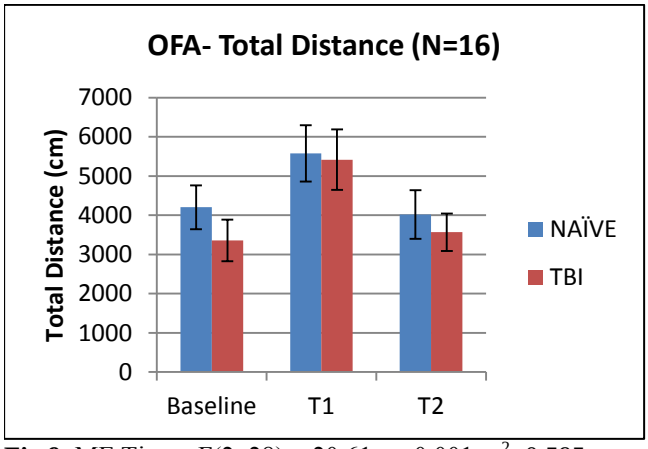

Fig.9. ME Time: $F(2, 28) = 20.61$, $p<0.001$, $\eta^2=0.595$; BL (3781.62 ± 232.24) = T2 (3793.32 ± 246.32) < T1 (5496.62 ± 280.30)
BL significantly different from T1 ($p<0.001$)
T1 significantly different from T2 ($p<0.001$)

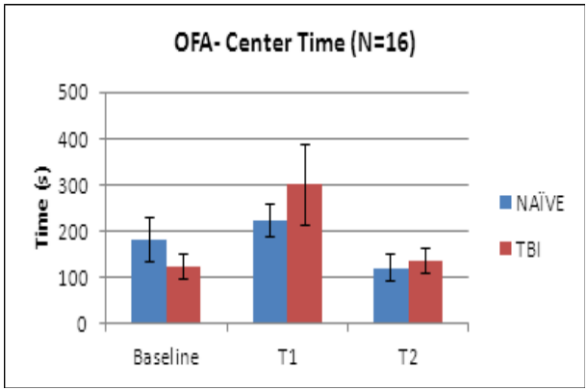

Fig.10. At 24 hr after injury, compared with baseline, animals took comparatively more time to escape, and by d7, it returned to normal.

- Animals receive 1 acclimation, baseline and 2 post injury measurements
- Animals are placed in the Open Field containers for 1 hour
- Variables analyzed: Total Distance, Horizontal Activity, Movement Time, Vertical Activity, Center Time, and Center Time as a proportion of Movement Time
- NOTE: Data from Cohort 1 has been removed from analyses due to equipment malfunction (collection of data stopped after 10-15 minutes). The issue was fixed prior to cohort 2 being started.

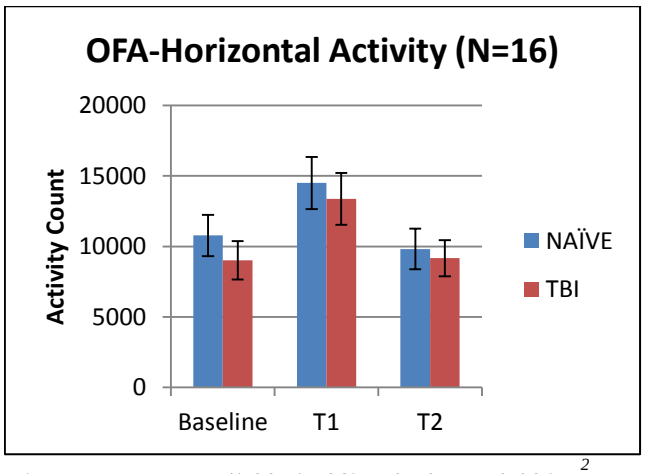

Fig.11.*ME Time: F(1.28, 17.88) = 25.24, p<0.001,* η^2 *=0.643; BL (9898.25 ± 592.16) = T2 (9494.75 ± 593.30) < T1 (13934.44 ± 630.*45)
BL significantly different from T1 (p<0.001)
T1 significantly different from T2 (p<0.001)

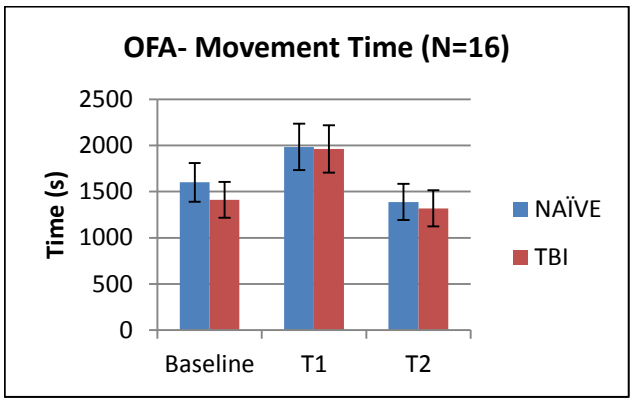

Fig.12.ME Time: F(1.23, 17.27) = 33.49, p<0.001, η^2 =0.705;
BL (1505.49 ± 72.19) = T2 (1353.23 ± 86.83) < T1 (1972.60 ± 75.94)
BL significantly different from T1 (p<0.001)
T1 significantly different from T2 (p<0.001)

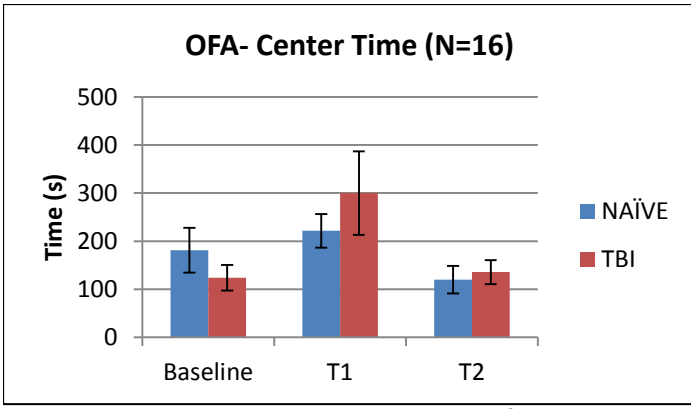

Fig.13. ME Time: F(2, 28) = 6.32, p=0.005, η^2 =0.3;
BL (152.5 ± 25.1) = T2 (127.8 ± 16.8) < T1 (260.7 ± 44.2)
BL significantly different from T1 (p<0.025)
T1 significantly different from T2 (p<0.010)

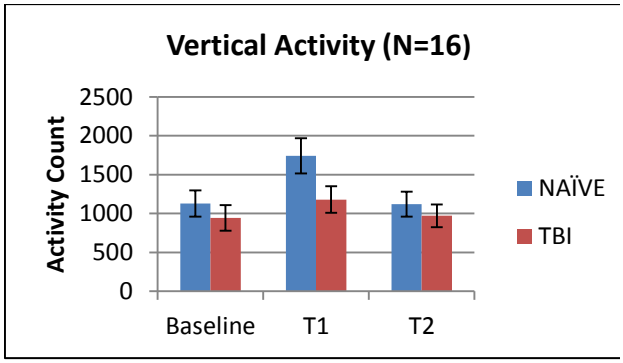

Fig.14. ME Time: F(1.37, 19.23) = 14.26, p=0.001, η^2 =0.505;
BL (1036.25 ± 85.28) = T2 (1046.56 ± 69.46) < T1 (1460.56 ± 73.16)
BL significantly different from T1 (p<0.001)
T1 significantly different from T2 (p<0.001)
ME Group: F(1, 14) = 7.27, p=0.017, η^2 =0.342;
Naïve (1330.71 ± 78.46) > TBI (1031.54 ± 78.46)
By Time:
ME Group at T1: F(1, 14) = 14.75, p=0.002, η^2 =0.513;
Naïve (1741.50 ± 103.46) > TBI (1179.63 ± 103.46)

Neurological Severity Scale – Revised

- Animals receive an NSS-R score for baseline and 2 post-injury observations
- NSS-R is 10 item test that looks at balance and simple reflexes
- Likert scale: 0 = normal response; 1 = partial and/or compromised response; 2 = no response
- Variables measured: Balance, drop, tail raise, drag, righting, ear reflex, eye reflex, sound reflex, tail pinch, and foot pinch

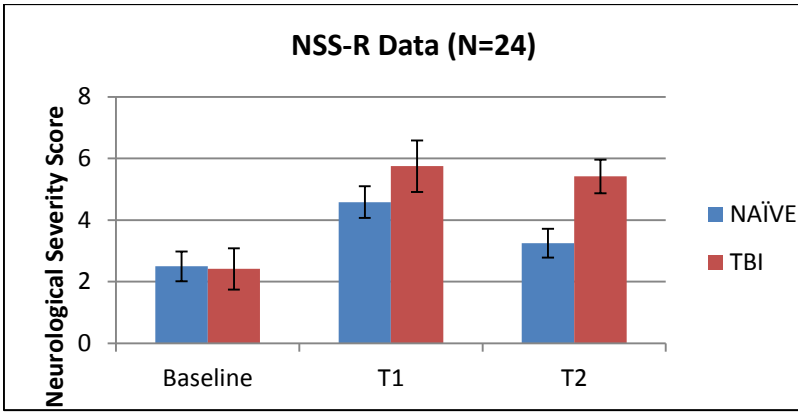

Fig.15. ME Time: $F(2, 44) = 13.22$, $p<0.001$, $\eta^2=0.375$;
BL (2.46 ± 0.41) < T1 (5.17 ± 0.49) = T2 (4.33 ± 0.36)
BL significantly different from T1 ($p<0.001$), T2 ($p=0.003$)
Just T1 & T2:
ME Group: $F(1, 22) = 5.93$, $p=0.023$, $\eta^2=0.212$;
Naïve (3.92 ± 0.48) < TBI (5.58 ± 0.48)
By Time:
ME Group at T2: $F(1, 22) = 9.23$, $p=0.006$, $\eta^2=0.295$;
Naïve (3.25 ± 0.50) < TBI (5.42 ± 0.50)
* No significant Findings when analyzed by change scores

Grip Strength

- Animals are tested using grip strength prior to injury (baseline) and receive 2 post-injury tests
- Animals are tested 3 times during the test day and the median score is used for analyses

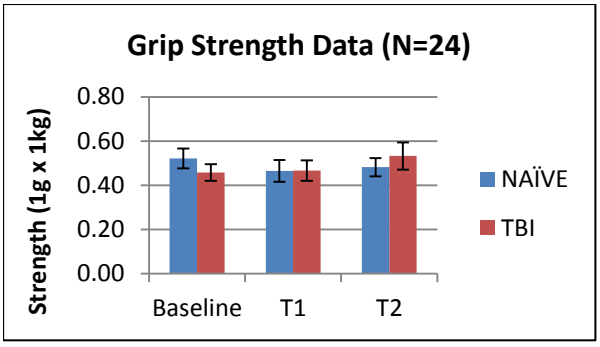

Fig.16. No Significant Findings

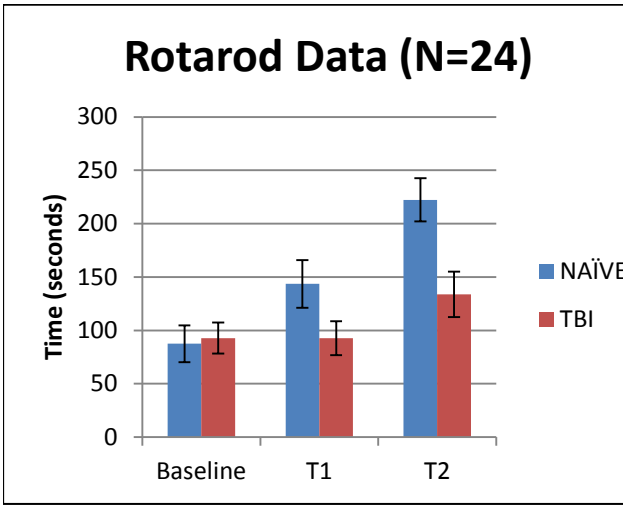

Fig.17

ME Time: $F(2, 44) = 16.04$, $p<0.001$, $\eta^2=0.422$;
BL (90.13 ± 11.26) = T1 (118.14 ± 13.71) < T2 (178.03 ± 14.68)

ME Group: $F(2, 44) = 5.39$, $p=0.030$, $\eta^2=0.197$;
Naïve (151.13 ± 13.63) > TBI (106.40 ± 13.63)
Significant Time **x** Group Interaction: $F(2, 44) = 4.43$, $p=0.018$, $\eta^2=0.168$;

By Time:

ME Group at T2: $F(1, 22) = 9.10$, $p=0.006$, $\eta^2=0.293$;
Naïve (222.31 ± 20.75) > TBI (133.75 ± 20.75)

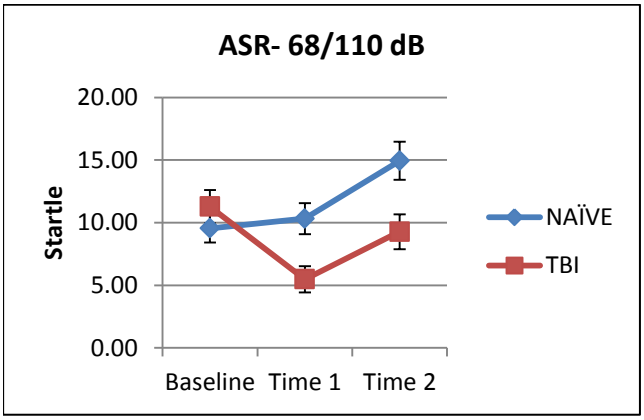

Fig.18. ME Time: $F(2, 44) = 7.85$, $p=0.001$, $\eta^2=0.263$;
BL (10.41 ± 0.87) = T2 (12.11 ± 1.03) > T1 (7.90 ± 0.81)
BL significantly different from T1 ($p=0.016$)
T1 significantly different from T2 ($p<0.001$)

ME Group: $F(1, 22) = 4.80$, $p=0.039$, $\eta^2=0.179$;
Naïve (11.60 ± 0.94) > TBI (8.68 ± 0.94)
Significant Time **x** Group Interaction: $F(2, 44) = 7.21$, $p=0.002$, $\eta^2=0.247$;

By Time:

ME Group at T1: $F(1, 22) = 8.99$, $p=0.007$, $\eta^2=0.290$;
Naïve (10.32 ± 1.14) > TBI (5.49 ± 1.14)

ME Group at T2: $F(1, 22) = 7.52$, $p=0.012$, $\eta^2=0.255$;
Naïve (14.94 ± 1.46) > TBI (9.28 ± 1.46)
* Also tested NSS-R Item #8 (Sound Reflex) and no significant differences at any time

Rotarod Test:

- Animals are tested prior to injury (baseline) and receive 2 post-injury tests
- Animals are tested 3 times during the test day and the average score is used for analyses

Acoustic Startle Response with Pre-Pulse Inhibition

- Animals receive 2 acclimation, baseline, and 2 post injury measurements
- Animals are placed in the Acoustic Startle chambers for 15 mins
- Data looks at a pulse alone (110 or 120 dB) as well as paired with a pre-pulse (68 or 82 dB)

Barnes Maze

- Animals are trained post injury (placing animal in escape hole for 30 seconds on first day of testing)
- Animals are tested 2 times/day for 5 consecutive days
- The average time it takes animals to find the target hole is used for analyses

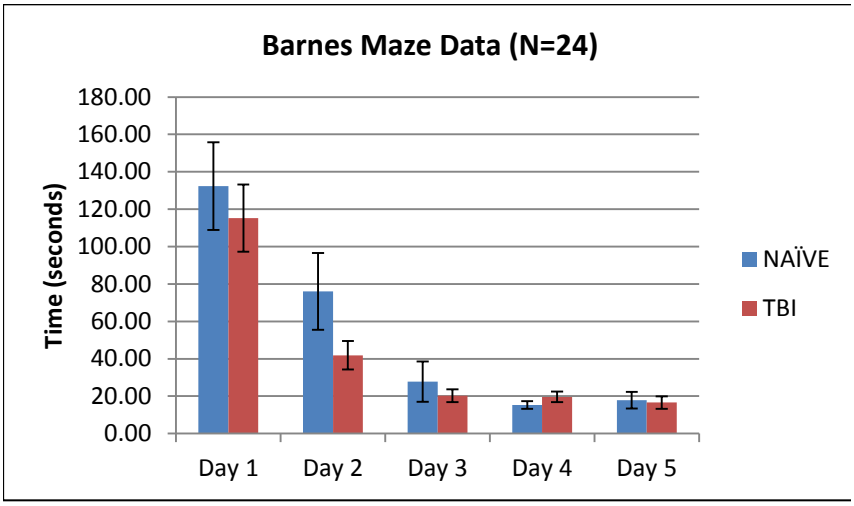

Fig.19. ME Time: $F(1.36, 13.61) = 14.10$, $p=0.001$, $\eta^2=0.585$;
Day 1 (98.08 ± 19.58) > Day 2 (42.63 ± 8.46) > Day 3 (14.63 ± 1.51) = Day 4 (17.46 ± 1.91) = Day 5 (17.21 ± 2.78)
Day 1 significantly different from Day 2 (p=0.027), Day 3 (p=0.001), Day 4 (p=0.002), Day 5 (p=0.002)
Day 2 significantly different from Day 3 (p=0.008), Day 4 (p=0.016), Day 5 (p=0.012)
Drop Day 5:
ME Time: $F(2.10, 46.16) = 32.42$, $p<0.001$, $\eta^2=0.596$;
Day 1 (123.81 ± 14.77) > Day 2 (58.96 ± 10.96) > Day 3 (24.02 ± 5.68) = Day 4 (17.44 ± 1.74)
Day 1 significantly different from Day 2 (p<0.001), Day 3 (p<0.001), Day 4 (p<0.001)
Day 2 significantly different from Day 3 (p=0.004), Day 4 (p=0.001)
By Time:
No significant findings

Summary of Neurobehavioral

OFA- Significant differences over Time (except CT/MT); T1 always higher than BL &T2

VA showed a significant difference between Group; Naïve showed more --VA than TBI animals (most prominent at T1)

NSS-R- Significant differences over Time; T1 & T2 were different from BL. Significant difference between Group; Naïve was lower than TBI animals (most prominent at T2)

GS- No Significant Findings

RR- Significant differences over Time; increase over time

-Significant differences between Group; Naïve higher than TBI

-Significant interactions showing that while both groups increased, TBI didn't increase as much as Naïve animals

ASR- 110 dB: Significant differences between Time, significant differences between Group (Naïve > TBI at both time points), significant interaction between Time and Group

– 120 dB: Showed similar findings over Time and interaction, but significant differences between groups only at T1

BM- Significant differences over Time; decreased over 5 days, but no differences between Group at any time point

h. Immunohistochemical Analysis

We have started immunohistochemical studies also in parallel with other studies. The protocol followed a method described earlier (Ariyannur et al., J. Comp. Neurol. 2010; 518 (15) 2952-2977) with minor modifications. With sufficient preparation and under general anesthesia, an intra-cardiac perfusion of neutral buffered formalin was done in rats (with or without TBI). The perfusion was assessed using the level of blanching of extremities and muscle rigidity. Brain was carefully dissected out after decapitation and kept in formalin for 24 hours and then transferred into a serial ascending concentration of sucrose, 10%, 20% and 30% in PBS, in order to cryopreserve the tissue, making it ready for cryosectioning. After mounting on a cryostat, the brains were sectioned. Each section was 20 µ think. The sections were directly mounted on a super frost charged glass slides and preserved in -80°C until further use. Fluorescence immunohistochemistry was done according to a method described earlier (Ariyannur et al. 2010), with minor modifications tailoring to specific primary antibody.

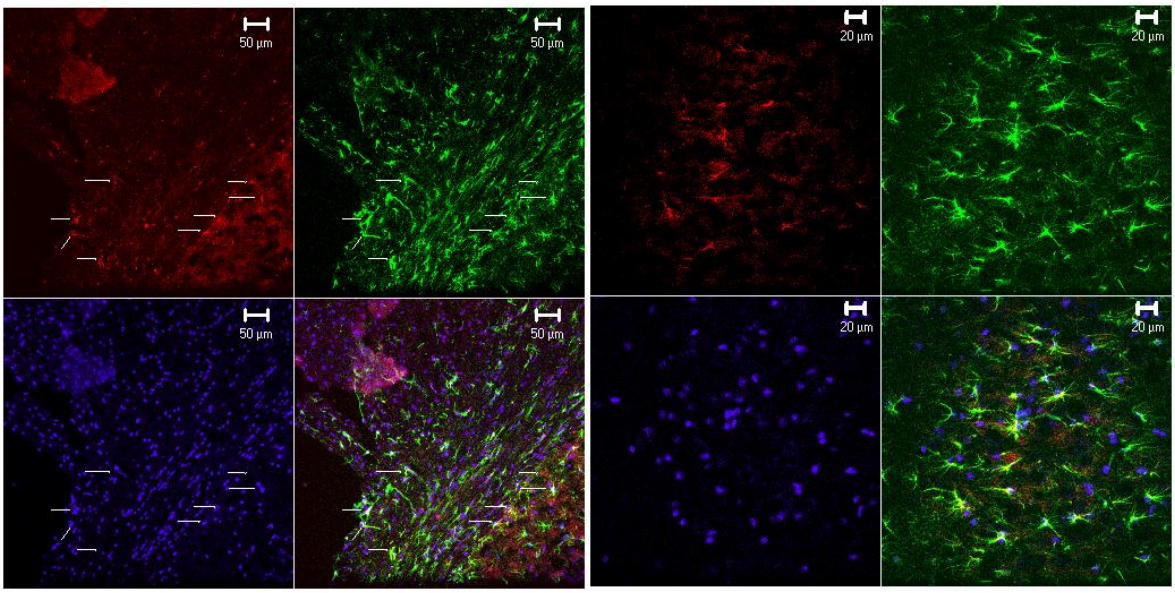

Fig 4: Immunohistochemical Colocalization of GFAP and Tau in post-TBI untreated rat forntal brain. Rat Anti-GFAP antibody (1:100) and Mouse Monoclonal anti-Tau antibody (1:100) was treated overnight with brain sections and developed with Green (for GFAP) and Red (For Tau) tagged secondary antibodies and Cell Nucleii was stained using DAPI. On the left side showes the perilesional cortex in 20x obj, and right side shows hippocampal CA1 and Dentate Gyrus obtained in 40x obj of Ziess Pascal LSCM. Arrows shows Colocalization for Green and Red fluorescence.

Immunohistochemical Studies to assess the effect of Traumatic Brain Injury

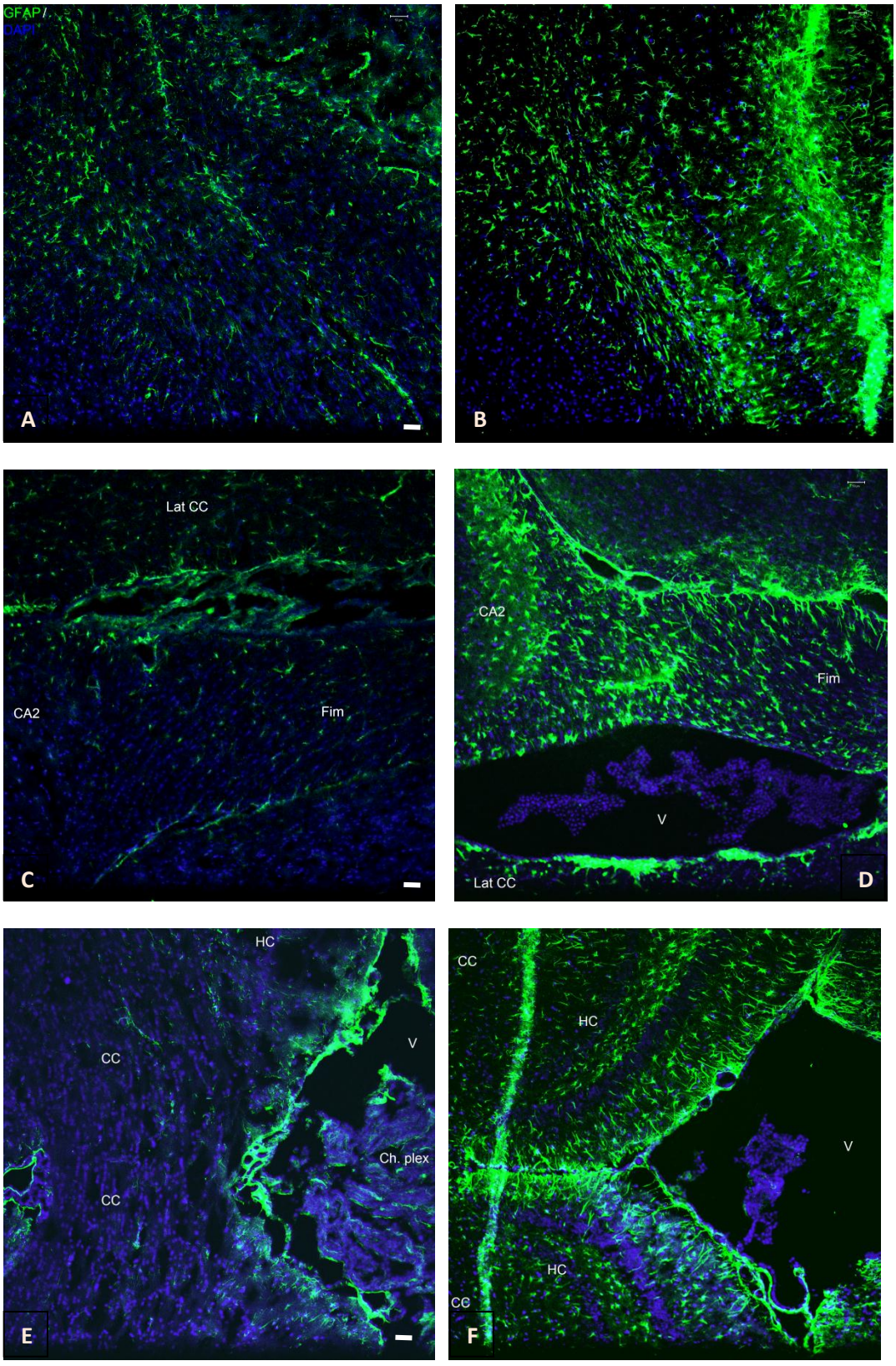

Figure 21: Comparison of GFAP immunolocalization profile in post TBI rat brain. Images A, C and E are untreated forebrain brain sections and image B, D and F are treated forebrain sections. Rat anti-GFAP (Invitrogen 13-0300) was used at dilution 1:100 overnight and used developed using Goat anti-rat IgG Alexa 488 giving green fluorescence. DAPI was used for nuclear staining giving blue fluorescence. Image A and B shows immunoreactivity profile (i.r.p) the mid-lateral corpus callosusm. Image C and D shows i.r.p in lateral hippocampal (CA2) area and fimbria of hippocampus (Fim); lateral ventricle (V) and lateral Corpus Callosum (Lat CC) are also shown. Image E and F show central callosal bundle (CC) and medial allocortex (HC) comparing the i.r.p of treated and untreated animals. Adjacent Choroid plexus and lateral ventricle are also shown. All are at 40x objective on PASCAL LSCM. 50u scale is shown at the right lower corner of A, C and E. The image B, D and F shows in general increased immunoreactivity to GFAP compared the image A, C and E in forebrain iso and allo cortex and corresponding white matter.

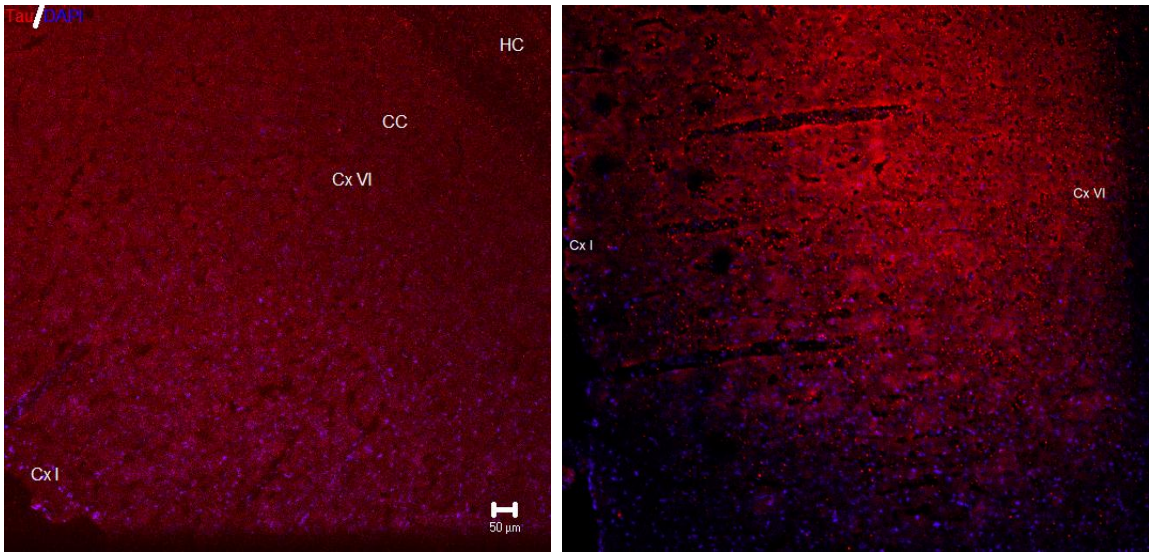

Fig.22. Depicted is the typical anti-Tau immunoreactivity in post TBI rat brain slices. Left image is from post TBI untreated animal and right image from post TBI Pyruvate treated animal. The red fluorescent punctate immunoreactivity (mouse Anti Tau dilution 1:50) and Goat anti mouse Alexa 594 at 1:100 dilution) which is non-colocalizing with DAPI is found across the tissue. The neocortical layers I through VI is shown with adjacent Corpus Callosum (CC) and hippocampus CA2 (HC). The punctate immunoreactivity is much higher in the treated compared to untreated sections. The intensity of ir is very low even at low dilution of antibody. Image is obtained in Ziess Pascal LSCM at 10x obj. The scale bar shown is 50um.

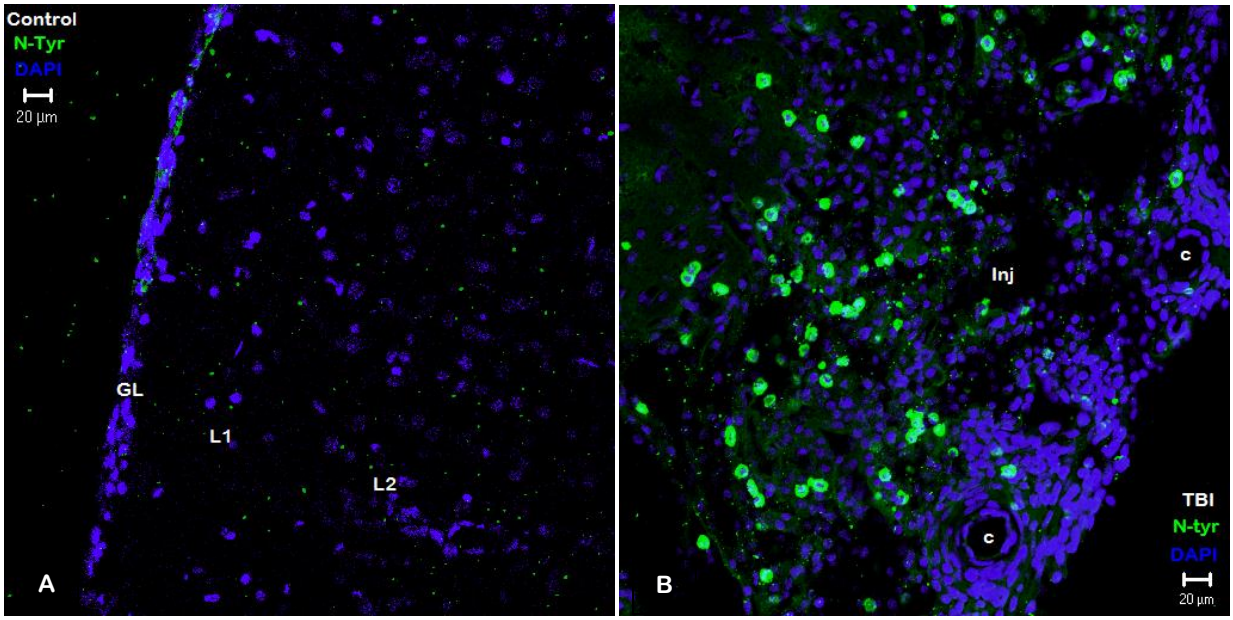

Figure 23: Nitro-tyrosine (N-Tyr) immunoreactivity in post injury cortical lesional areas (B) compared to uninjured iso-cortex (A). Mouse Anti Nitro-tyrosine was used (1:100) incubated overnight and developed using Goat Anti-Mouse Secondary antibody coupled to Alexa 488 ® giving green fluorescence. The cell nuclei are stained using DAPI giving blue fluorescence. The images were viewed in Laser Scanning Confocal Microscope (Zeiss- Pascal) using 20x obj. and edited using Zeiss Image Examiner Ver 5.0. The iso-cortical pyramidal layers 1 and 2 are seen in the field (depicted in the picture as L1 and L2) and the ensheating glial limitans (dense DAPI nuclear stained layer "GL" in the picture), an astroglial cell layer adjacently beneath the pia-mater. In the uninjured control cortical sections, the GL is intact, as well as L1 and L2. The N-Tyr immunoreactive cells were virtually absent in injured control sections. While there were a large increase in scattered density of N-Tyr immunoreactive cells in the peri-lesional cortical sections (marked as Inj in the image) after one week post-injury. Note that instead of GL, there is a large increase in cell density in the peri-lesional areas associated with blood capillaries (c). The presence of active Nitro-tyrosine immunoreactive cells suggests the presence of reactive oxygen (ROS) and nitrogen (RNS) free radical species in the peri-lesional cortex and its impact in the cell damage and proliferation. The amount of impact of these ROS and RNS are evident even after seven days post injury in rat brain.

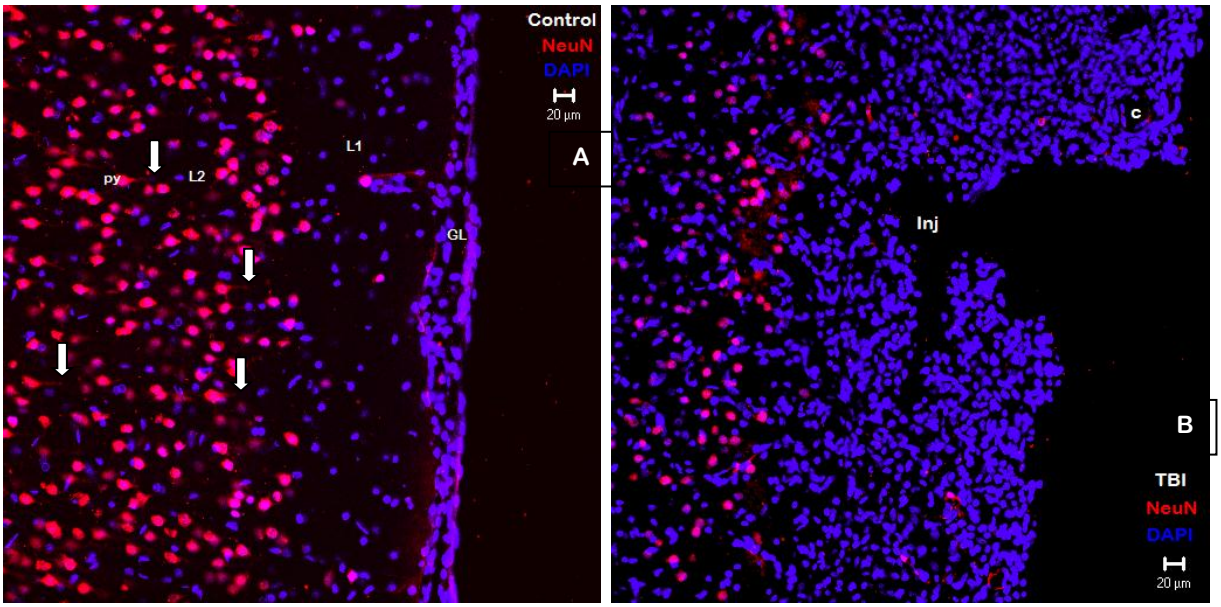

Figure 24: Comparison of NeuN immunoreactivity in TBI (B) vs. control (A) rat brain sections. Mouse Anti-NeuN antibody (1:100) was incubated overnight with the brain sections and developed using Goat anti-Mouse IgG coupled to Alexa 594 ® giving a red fluorescence. DAPI was used for nuclear staining. The experimental details of the TBI are given elsewhere. The image was acquisition details are given in the figure legend 1. In Cortical Layer 1 and 2 (depicted as L1 and L2), the terminally differentiated neurons are intensely immunoreactive to Neuronal Specific Nuclear Protein, NeuN[1]. Image A shows typical NeuN immunoreactivity. In post-mitotic neurons, NeuN shows an intense, but non-uniform nuclear immunoreactivity (giving variegated red and pink appearance due to non-uniform colocalization with DAPI nuclear staining as in the image A). Also, perhaps more importantly, a lighter NeuN immunoreactivity is seen in the neuronal cytoplasm and especially apical dendrites of pyramidal neurons (white arrows), which facilitates the identification of the pyramidal cell morphology in the outer pyramidal cell layer of neo-cortex (see picture A, depicted as py). Cortical Pyramidal neurons are one of the several selected neuronal sub-types of CNS neurons which are well-known for their extra-nuclear immunoreactivity to NeuN[2]. On the otherhand, image B shows the NeuN immunoreactivity in the same cortical areas after TBI. Note that the outer glial cell layer (GL) DAPI is absent due to the impact injury. Instead, a diffusely loose cellular layer with newly formed capillaries (depicted as "c" in the image B) is seen. The NeuN immunoreactive cells are conspicuously sparse in the image B. The individual cells which does have NeuN immunoreactivity shows a lower intensity and without a cytoplasmic or dendritic staining. Moreover, instead of the typical variegated appearance of nuclear immunoreactivity, there is a uniformly lower immunoreactivity suggesting DNA clustering and high packing density in these cell types implicating apoptotic changes. Images were acquired using same 20x obj. and the sizes of the cells are comparable to each other. Also, a scale bar is shown in each image for size comparison. This immunoreactivity pattern was consistent across three different animals in each of the group.

[1] Mullen RJ et al., *Development.* 116(1):201-211 (1992)
[2] Lind D et al., *J. Neurosci. Res.* 79:295-302 (2005)

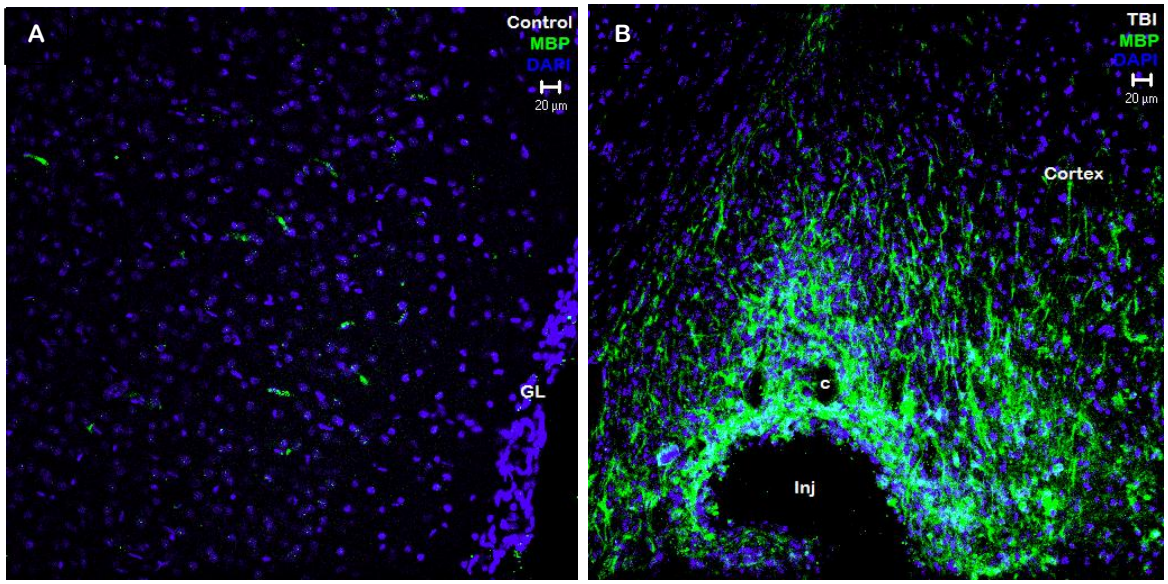

Figure 25: Effect of impact injury on MBP immunoreactivity in cortical peri-lesional areas. Myelin Basic Protein (MBP) is an oligodendrocytes specific marker protein which is found in the ensheathing layers of myelin. Typically, the superficial cortical layers have very less myelin compared to sub-cortical areas and white matter bundles such as corpus callosum. We used Anti-Rabbit MBP (1:1000) and developed using Green fluorescent Alexa 488 ® coupled Goat Anti-rabbit secondary antibody. The images were captured using a Zeiss-PASCAL LSCM. The expression is much higher in the post TBI superficial layers compared to control as seen by the amount of green fluorescence in the picture on the right side. We found a large increase in the MBP immunostaining in the post injury peri-lesional cortex compared to the naïve cortical sections. Like GFAP for astrocytes, MBP is a cellular marker for oligodendrocytes and its higher immunostaining signifies the proliferation of oligodendrocytes in these peri-lesional areas. Since the impact injury was 7 days prior, this explains more oligodendrocytes recruitment. The impact injury has made a contused indentation in the immediate cortex making a deep recess in the tissue marked "inj" in the image B. The MBP staining is characteristically found in the cellular structures as well as fiber structures in the peri-lesional cortex, unlike the typical strand like staining appearance (see A). This might also suggest and increased expression of MBP in the immediate peri-lesional cortex. But the Anti-rabbit antibody is against a synthetic peptide which is a fragment of the whole protein. So technically the anti-body may not be able detect the whole protein per se. Also, one previous report says that, there is an extensive degradation of MBP following TBI.[3] So the increased expression shown might be increased degradative product of MBP. But no other report is available regarding the whole MBP expression in post-injury; it might very well be an increased expression of MBP in the peri-lesional areas as a reparative process. Further studies are required to characterize the MBP expression and degradation in post-injury paradigms.

[3] Liu MC et al., *J. Neurochem*. 98(3): 700-712 (2006).

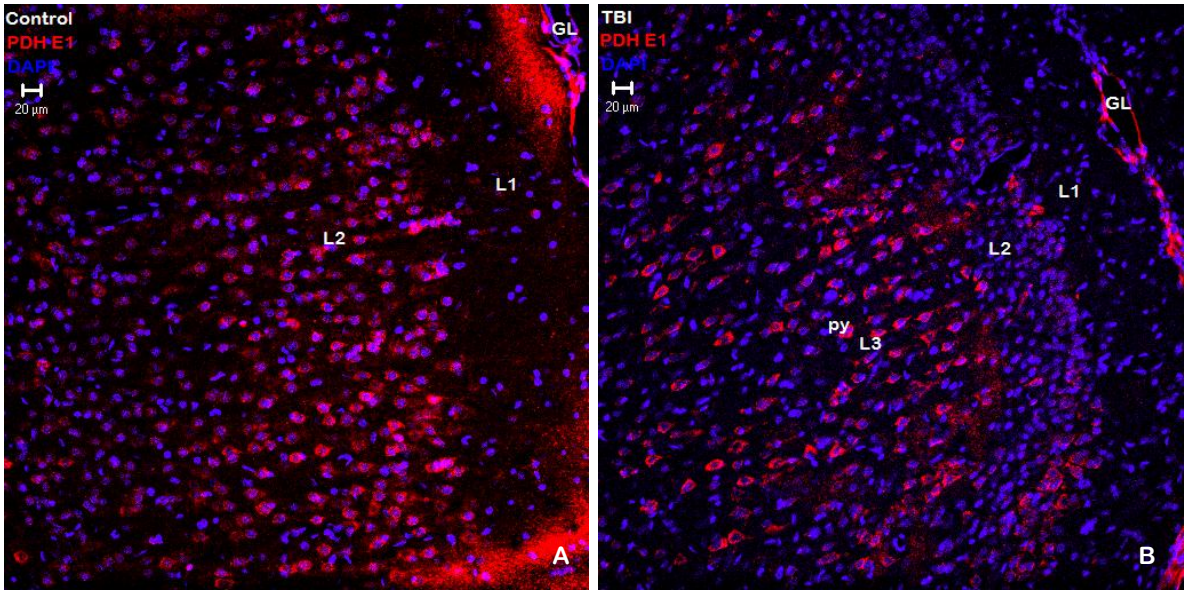

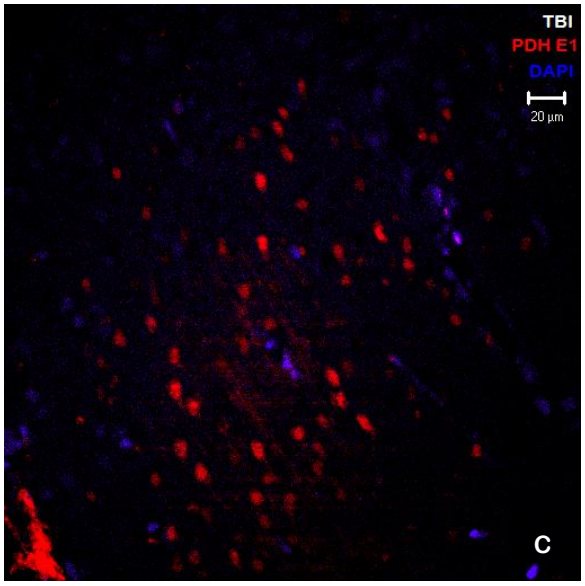

Figure 26: Comparison of PDHE1-α immunoreactivity in TBI (B) vs. naïve (A) rat cortical brain sections. Image C is from the contused brain area overhanging the normal tissue. Mouse PDHE1α (1:100) was incubated overnight with the sections and Goat Anti-mouse Alexa 594® was used to give red fluorescence. DAPI was used for nuclear staining. L1, L2 and L3 are the pyramidal cell layers of the neo-cortex. Glial limitans (GL) and outer pyramidal cells are also shown. Both the tissues and sections were treated under same condition except the injury. The red fluorescence is mainly seen in the neuronal cell types than astroglial cells. The extra-nuclear immunoreactivity of PDHE1α is characteristic. The apical dendrities and cytoplasm of the pyramidal neurons are well seen showing typical triangular appearance in both images A & B. Image C shows different pattern of PDHE1α immunoreactivity. It is uniformly distributed in the cells, and there is lower level of density and denser staining and comparatively smaller cells compared to cells of naïve brain sections or peri-lesional injured brain areas. The cells are pyknotic and very less DAPI stain. This might suggest that he PDHE1 α may not have a drastic change in seven day post-injury. Certainly, the contused brain areas might have very less level of expression. Images A and B was acquired from a 20x obj. while Image C was obtained using a 40x obj. Scale bar is given inside the images for size comparison.

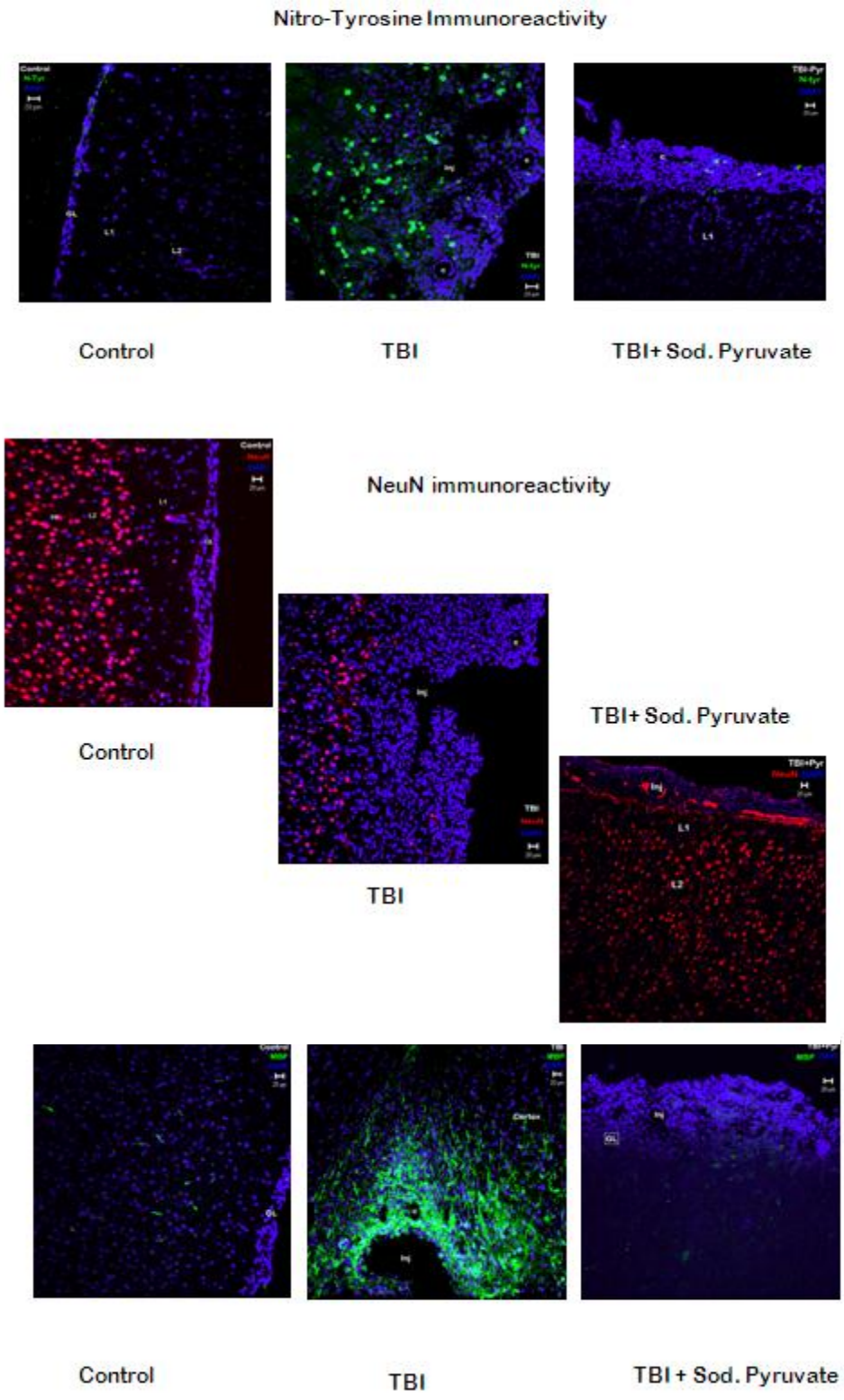

Fig.27. Mouse NeuN 1:100; Alexa 488® 1:100. Rabbit HIF (PAB-1) 1:300, Alexa 594 1:100. DAPI. **Upper Picture Panel:** Control PTSD. Cortex Layer 1-2. Glial limitans showing linear DAPI staining pattern. Arrow on the right figure shows the colocalization of NeuN and DAPI in layer 1 py. Neurons. **Lower Picture Panel: PTSD+TBI.** Pericontusional Cortex. Large increase in HIF+ cells in the peri contusional areas is shown. High magnification shows punctate cytoplasmic immunoreactivity in specific cells which are larger in size compared to other cell types, extranuclear to adjacent small pyknotic nucleus.

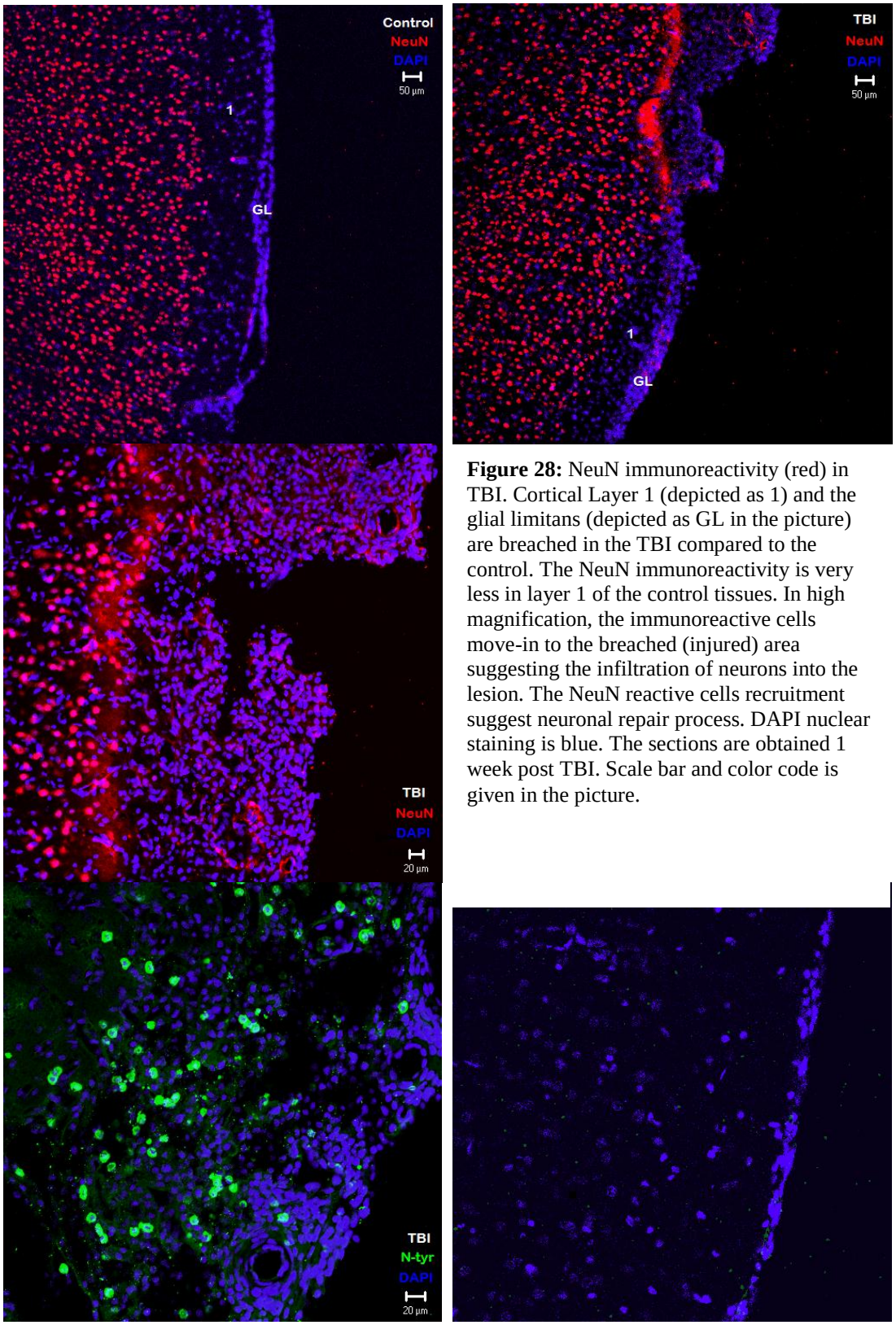

Figure 28: NeuN immunoreactivity (red) in TBI. Cortical Layer 1 (depicted as 1) and the glial limitans (depicted as GL in the picture) are breached in the TBI compared to the control. The NeuN immunoreactivity is very less in layer 1 of the control tissues. In high magnification, the immunoreactive cells move-in to the breached (injured) area suggesting the infiltration of neurons into the lesion. The NeuN reactive cells recruitment suggest neuronal repair process. DAPI nuclear staining is blue. The sections are obtained 1 week post TBI. Scale bar and color code is given in the picture.

Fig.29. Obvious Nitro-tyrosine immunoreactivity (Green) in lesion compared to uninjured control

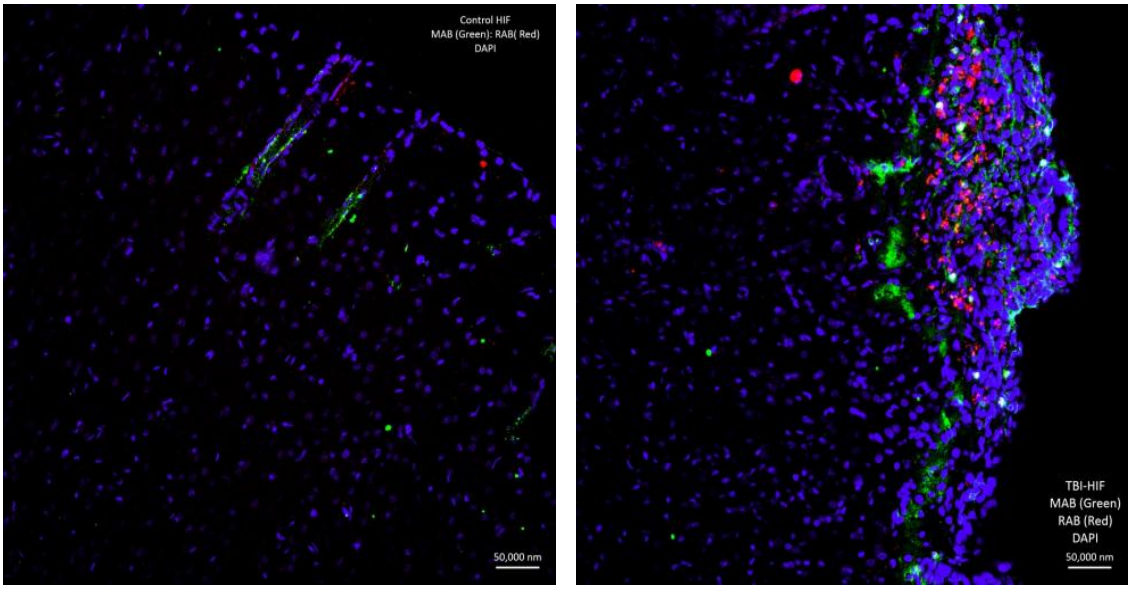

Cortical/Peri-lesional HIF Immunoreactivity Control vs. TBI

Green: HIF Mouse Monoclonal Antibody (1:300); IgG Alexa 488® (1:100)
Red: Rabbit polyclonal Antibody (1:300); IgG Alexa 594 ® Blue; DAPI
left image: Uninjured Control. Very less immunoreactivity except less intense cortical peri-capillary immunoreactivity in control tissues.
Right image: Intense immunoreactivity at the perilesional cortex. Both the antibodies shows large increase in immunoreactivity
Images are obtained at 20x obj. from Zeiss Confocal Microscope.
Scale bar is given at the bottom of the image for size comparison.
More details in the next slide.

Fig.30. HIF immune reactivity in control vs. TBI

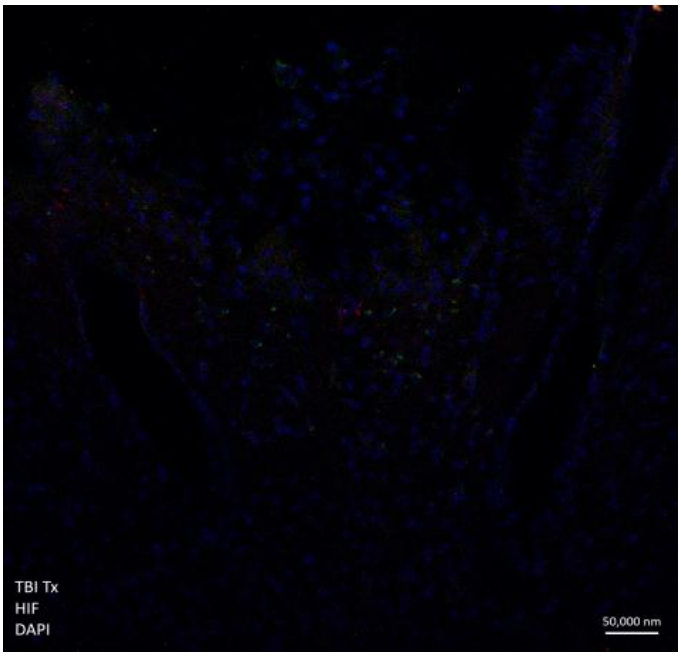

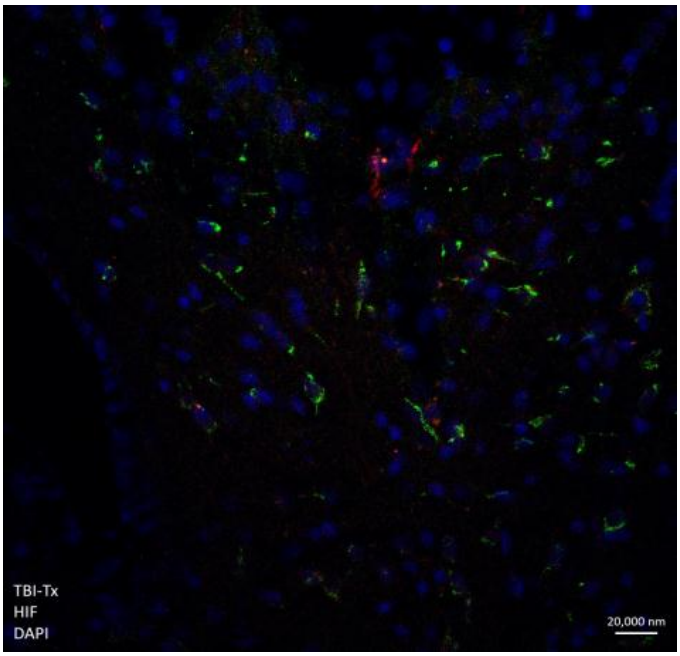

HIF Immunoreactivity in TBI with Sod. Pyruvate treatment

Left side image 20x obj. and right side image from 40x obj. The antibody and fluorescent marker are same as given in previous slide. But the immunoreactivity pattern is drastically different in these sections compared to earlier two groups. In general the HIF immunoreactivity was found to be lesser than the TBI untreated group. But the cytoplasmic localization of the lesional areas are more or less preserved. But the nuclear immunoreacitvty is markedly reduced in the pyruvate treated tissue sections compared to untreated group. This suggests that the transcriptional regulatory role of HIF on hypoxia responsive elements is very low with Sodium pyruvate treatment. On the otherhand, the cytoplasmic expression is maintained at moderate levels which means the normoxic cell types are more preserved. This implicates that the higher presence of normoxic cell types in the peri-lesional cell types suggests the protective role of sodium pyruvate.

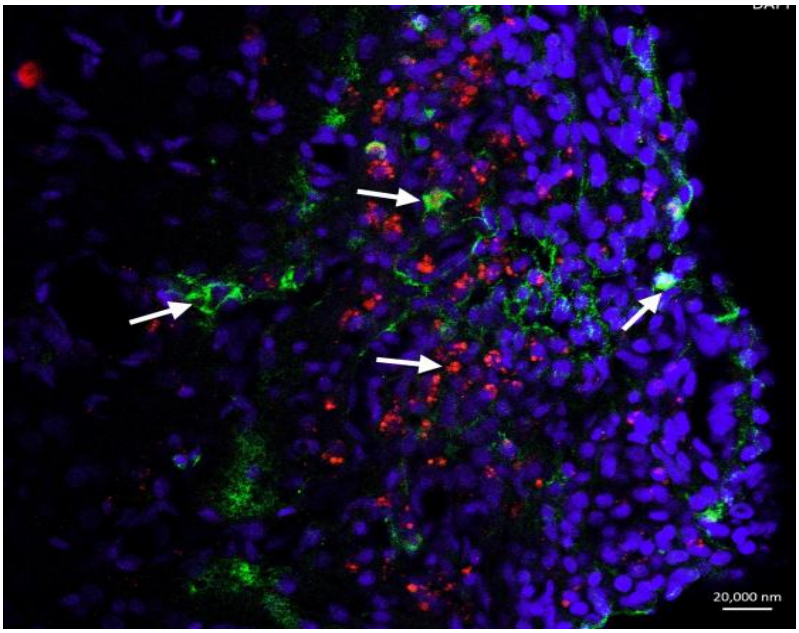

Peri-lesional HIF Immunoreactivity

onoclonal anti HIF Antibody (MAB) is present more intensely in peri-nuclear areas o as, it was less intensely localized and retained peri-capillary immunoreactivity in th cesses of the newly recruited cells inside the contused tissue is well shown in this p ber of cyplasmic stained cells suggests the newly derivded/recruited cell types.

Anti-HIF antibody (RAB) showed a different immunoreactivity pattern. RAB showed calization, with very minimal cytoplasmic staining. Characteristic clump like pattern suggests the transcriptional coactivating effect of HIF in hypoxia induced cells.

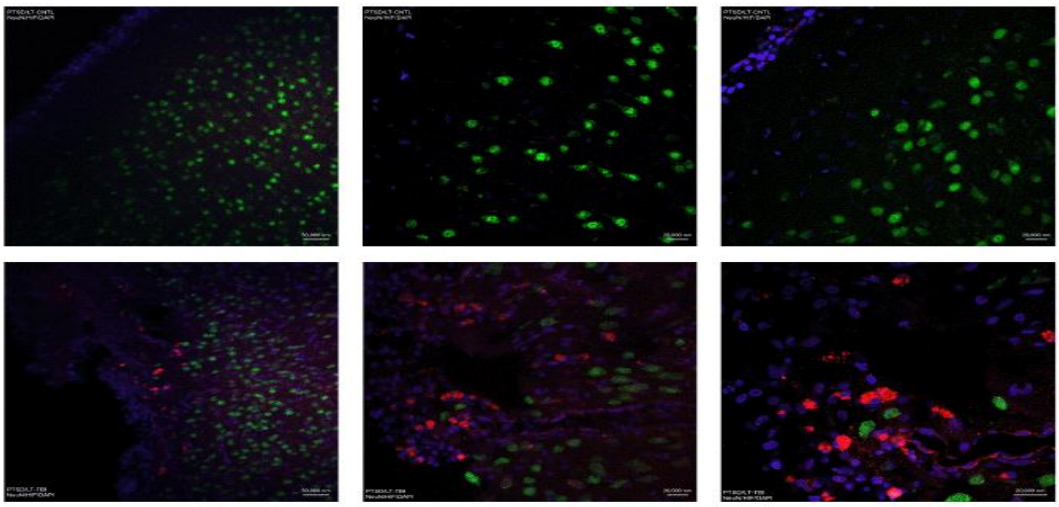

Fig32. Evaluation of slides is under progress

i. Cytokine Array of Sera samples of Control vs. post TBI rats:

Cytokine array was done using Rat specific Antibody microarray (RayBio® Rat Cytokine Array II) in Control and post TBI rat sera after one week post injury. Equal amount of sera was taken and was diluted 10 times. The Array membranes were treated with blocking buffer for 2 hours in room temperature and then incubated with the diluted sera sample for 2 hours at room temperature. The membranes were washed three times with Wash buffer 1 and two times with wash buffer 2, each for 5 min. The membranes with treated with primary antibody for overnight at 4°C. The membranes are washed again and treated with secondary antibody for 2 hours at room temperature. After washing, the membranes were developed using Chemiluminiscent detection reagents in the kit and images acquired using BioMax X-ray film or FUJI Imager (FLA 3100). The images in X-ray film was scanned using a flat bed scanner (FUJI Image scanner/Canon Multifunctional Scanner). The images were analyzed using FUJI ImageQuant.

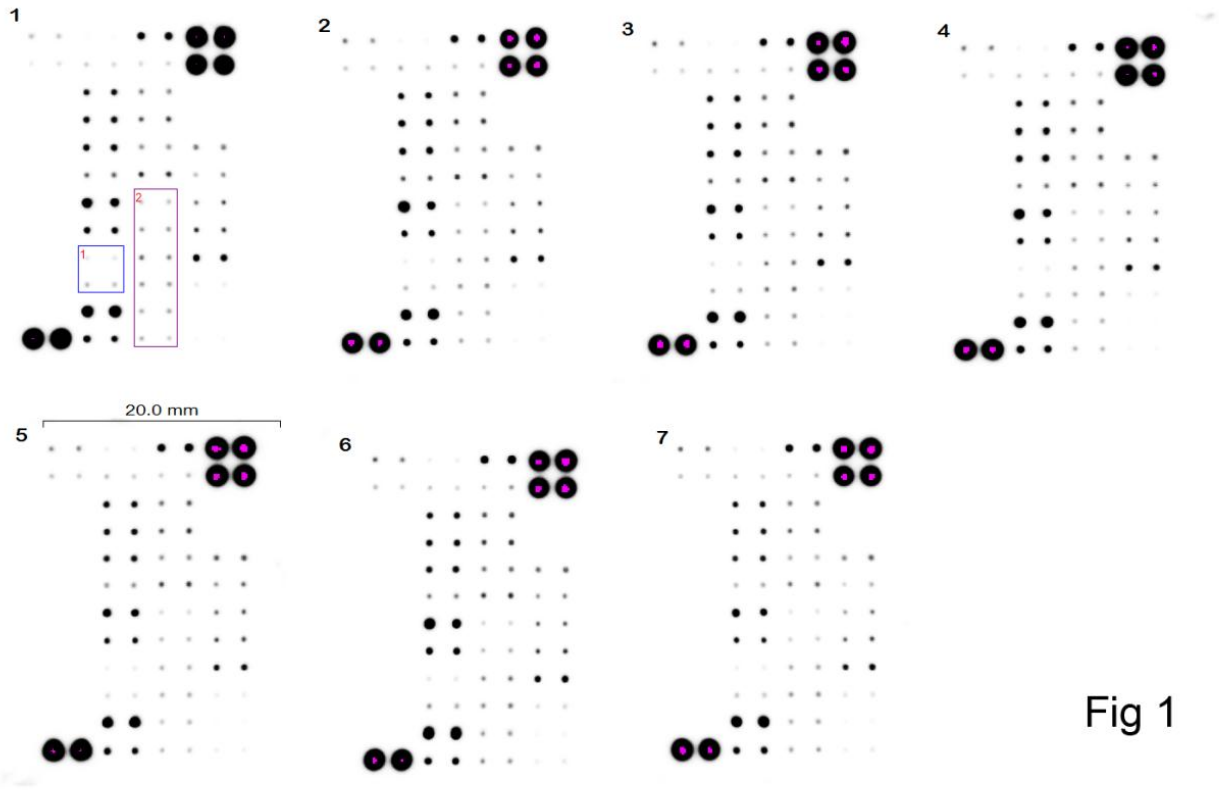

Figure 33: A typical Cytokine microarray image from sera of rats with or without TBI is shown. The number on the top left hand corner corresponds to each membrane which contains one sample. Each number is same as the animal identification number. Numbers 1 through 4 represent the samples of TBI animals and 5 through 7 represent that of Naïve. For comparison across the animals, the spots which are inside the two squares (blue and pink) can be compared. The intensity of the spots is higher in TBI samples compared to Naïve.

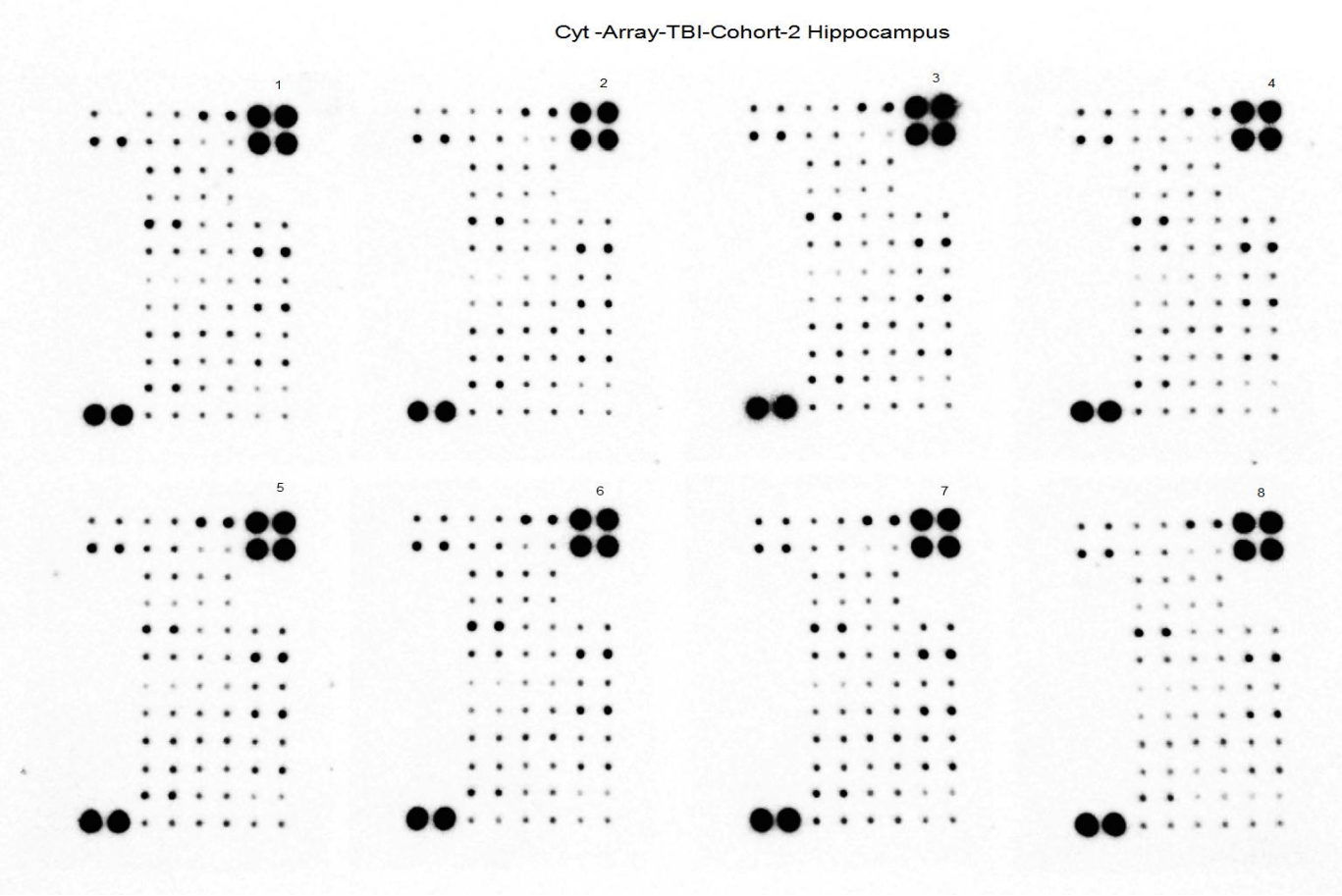

Figure.34. A typical Cytokine microarray image from the hippocampus of rats with or without TBI is shown. The number on the top left hand corner corresponds to each membrane which contains one sample. Each number is same as the animal identification number. Numbers 1 through 4 represent the samples of TBI animals and 5 through 7 represent that of Naïve. For comparison across the animals, the spots which are inside the two squares (blue and pink) can be compared. The intensity of the spots is higher in TBI samples compared to Naïve.

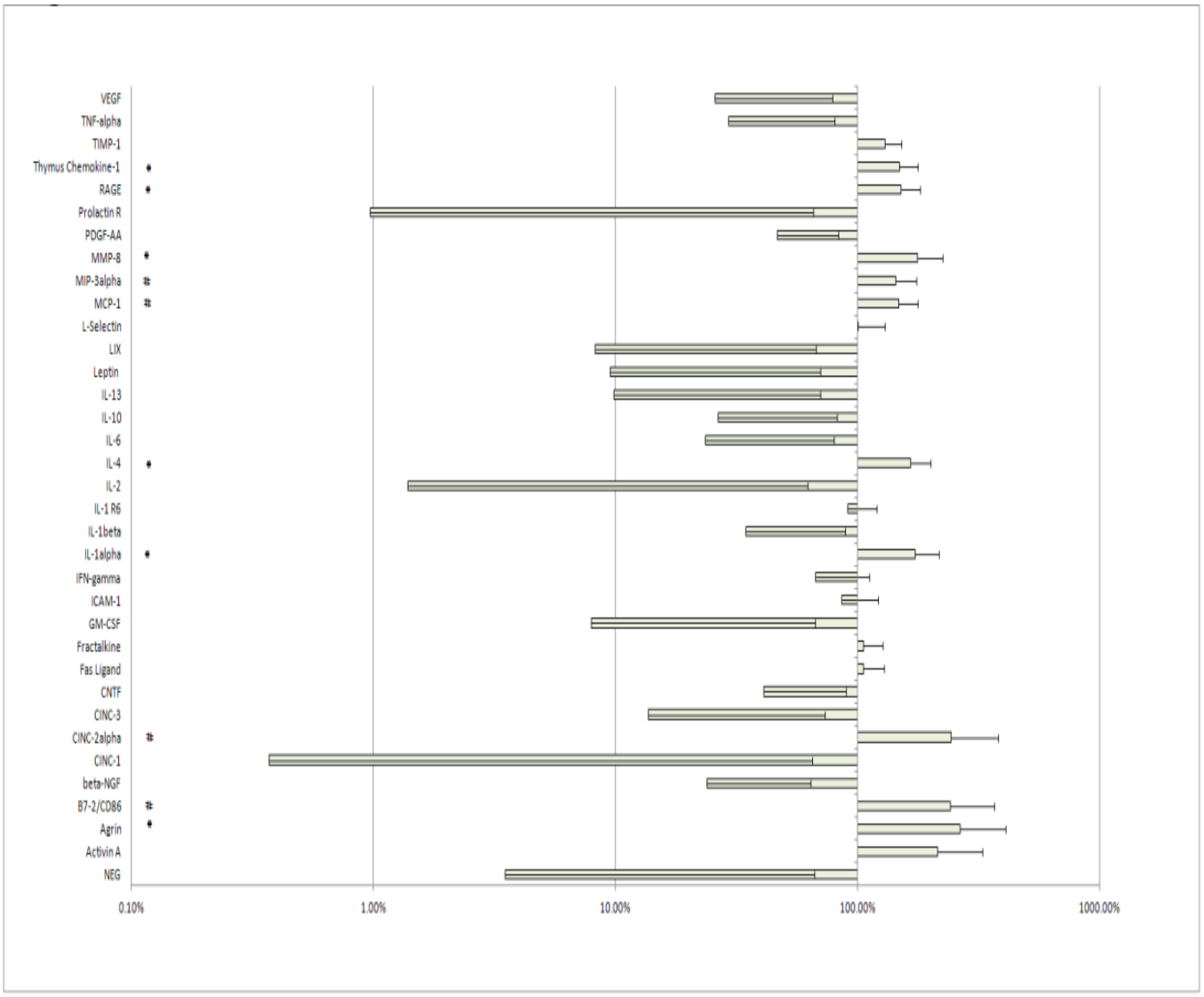

Figure 35: Sera anti-cytokine array. The expression of different cytokines in the sera of injured rats compared to Naïve is depicted in this figure. The data is presented as percentage difference from control in a log scale where 0.00% is the value of the Naïve. Error bar is the S.E of percentage calculated using Taylor series approximation, E. C. Fieller method (Ref). The * shows significant change ($p < 0.05$) from the control using randomized block ANOVA with experiment as a blocking factor was done in order to adjust for the difference between the experiments. The values are from eight animals in each Naïve and TBI group. The markers with # sign are marginally significant ($p<0.1$).

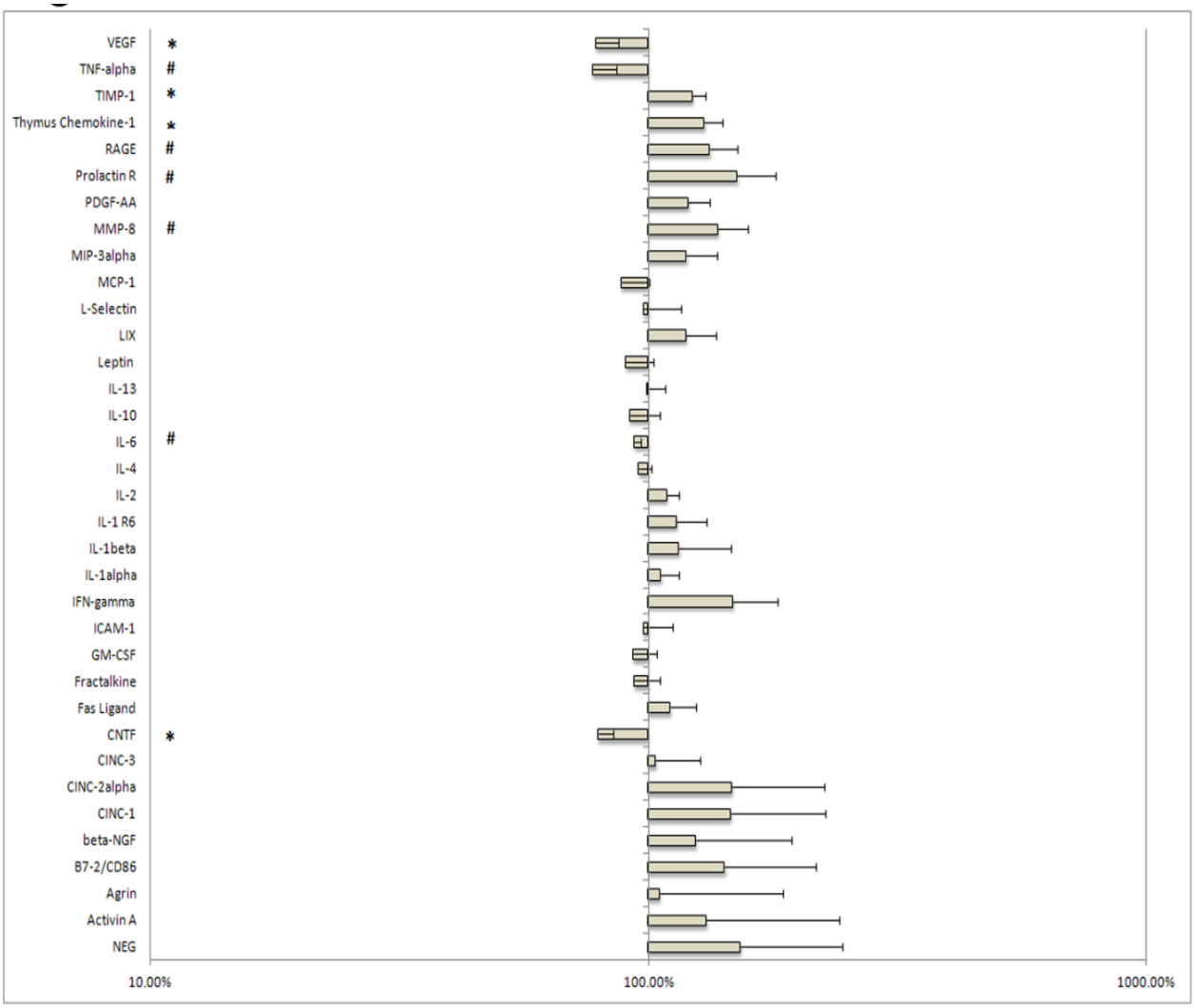

Figure 36: Array of hippocampal tissue homogenate. The normalized value of the control is represented at 100%. The percentage range from the normal value is depicted as bar graph on either side of the control. Each bar graph is for each cytokine marker. Five parameters are significantly different at 95% confident interval and 10 parameters are significantly different at 90% C.I. The statistics was done exactly like the serum (blocked ANOVA) with experiment as the blocking factor. The trend is represented here as a log graph of the percentage difference in cytokine expression in TBI compared to Naïve. See the method section for detailed explanation of experiment and method of analysis. The asterisk sign (*) shows the significant difference in TBI group compared to Naïve ($p \leq 0.05$). The pound sign (#) denotes marginally significant parameters ($p \leq 0.1$).

Array of hippocampal tissue homogenate. Five parameters are significantly different at 95% confident interval and 10 parameters are significantly different at 90% C.I. The statistics was done exactly like the serum (blocked ANOVA) with experiment as the blocking factor. The trend

is represented here as a log graph of the percentage difference in cytokine expression in TBI compared to Naïve. So 100% is the normalized value of the control and the deviation from that line is depicted as bar graph for each cytokine marker.

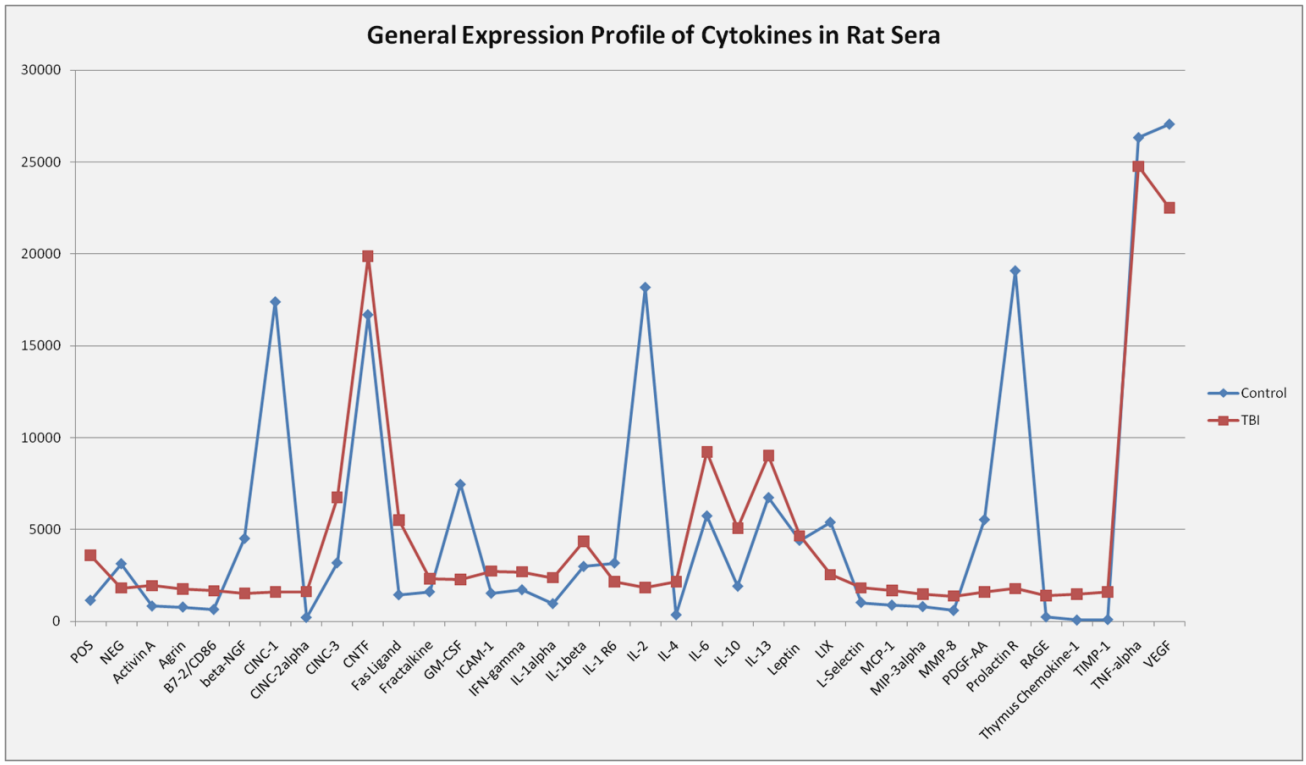

Figure 37: The expression profile of 34 Cytokine marker signals from the sera of injured and uninjured rats is compared. The red spots depict the expression levels of inflammatory markers in the post TBI sera and blue spots represent that of the control. The results are the mean expression intensity of five rats in each of the group. As seen in the picture, there was trend of decrease in expression of β-NGF, CINC-3, GM-CSF, IL-2, PDGF-AA, Prolactin-R, TNF-α and VEGF in TBI group compared uninjured controls. See the tabular column detailing the description of the cytokine markers and their significance. This trend was conspicuous because of another fact that there was a protracted increase with other markers other than those mentioned above. The general trend with this comparative Cytokine expression study in control and TBI group certainly suggests that these specific markers could be further studied to identify their validity for identifying the brain injury, both qualitatively and quantitatively.

Table 4.

Changes in cytokine expressions in response to TBI and their role in cell survival

Cytokines	Increased (↑)or Decreased (↓)in TBI compared to Control	Significance
β-NGF	↑	Neuronal specific growth factor
CINC-3	↑	Pro-inflammatory: Neutrophil chemo-attractant[4]
FasLigand	↑	Pro-apoptotic: Attaches to Fas-FasR
GM-CSF	↓	Pro-inflammatory: Macrophage induction
IL-1β	↑	Pro-inflammatory: Lymphocyte mitogen
IL-1 R6	↓	Pro-inflammatory: CNS and vascular binds to 1L-1α[5]
IL-6	↑	Pro-inflammatory: vascular smooth muscle contraction; Anti-inflammatory: inhibits TNF-α
IL-10	↑	Anti-inflammatory: inhibits Th1 specific cytokine expressions and NF-κB activity
IL-13	↑	Pro-inflammatory allergic reactions: binds to IL-4
LIX	↓	Pro-inflammatory: LPS inducible CXC chemokine ligand5 (TNF-α induced)
PDGF-AA	↓	Mitogen/Anti-apoptotic : Homodimeric proteins binds to TK-receptor
Prolactin-R	↓	Growth Factor: Prolactin binds, [6]
TNF-α	↓	Pro-inflammatory: multiple functions
VEGF	↓	Angiogenesis and Growth Factor

[4] Takano K et al., *Inflamm Res*. 2001 Oct;50(10):503-8.
[5] Lovenberg TW et al., *J Neuroimmunol*. 1996 Nov;70(2):113-22.
[6] Ali S et a., *J Biol Chem.* 1998 Mar 27;273(13):7709-16.

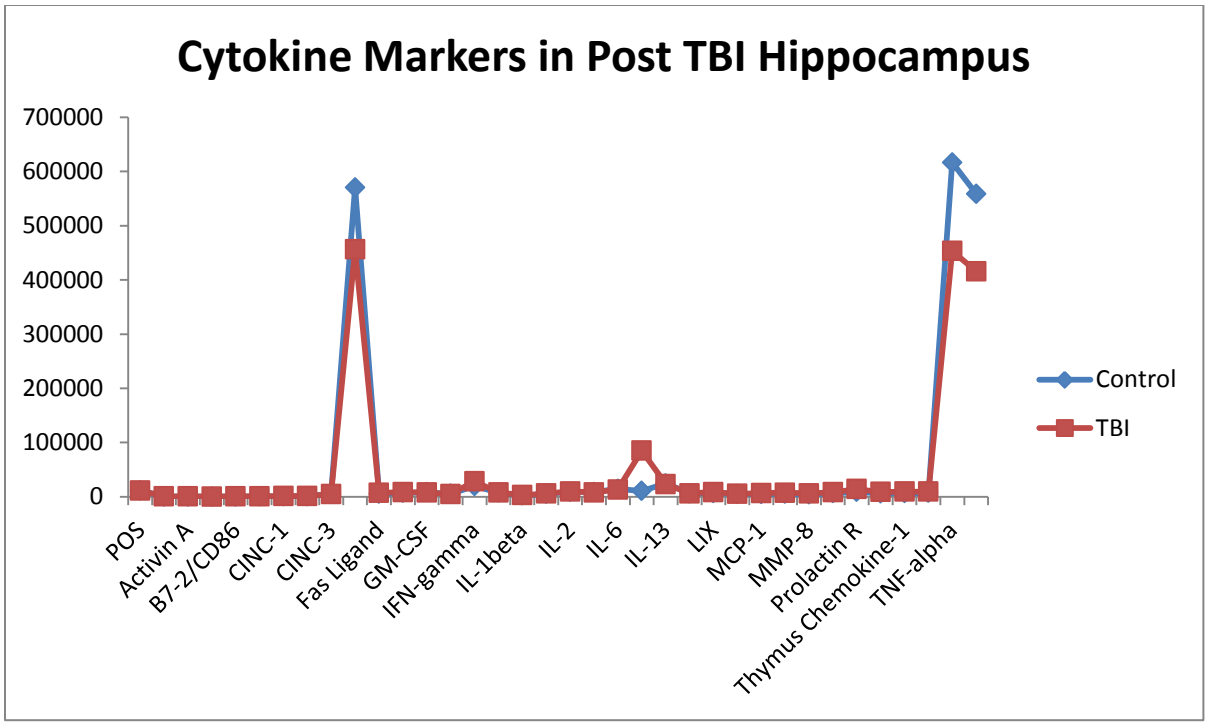

Figure 38: General Trend of Expression Profile of Cytokines in RatHippocampus: Control is from five rats and TBI from seven rats.

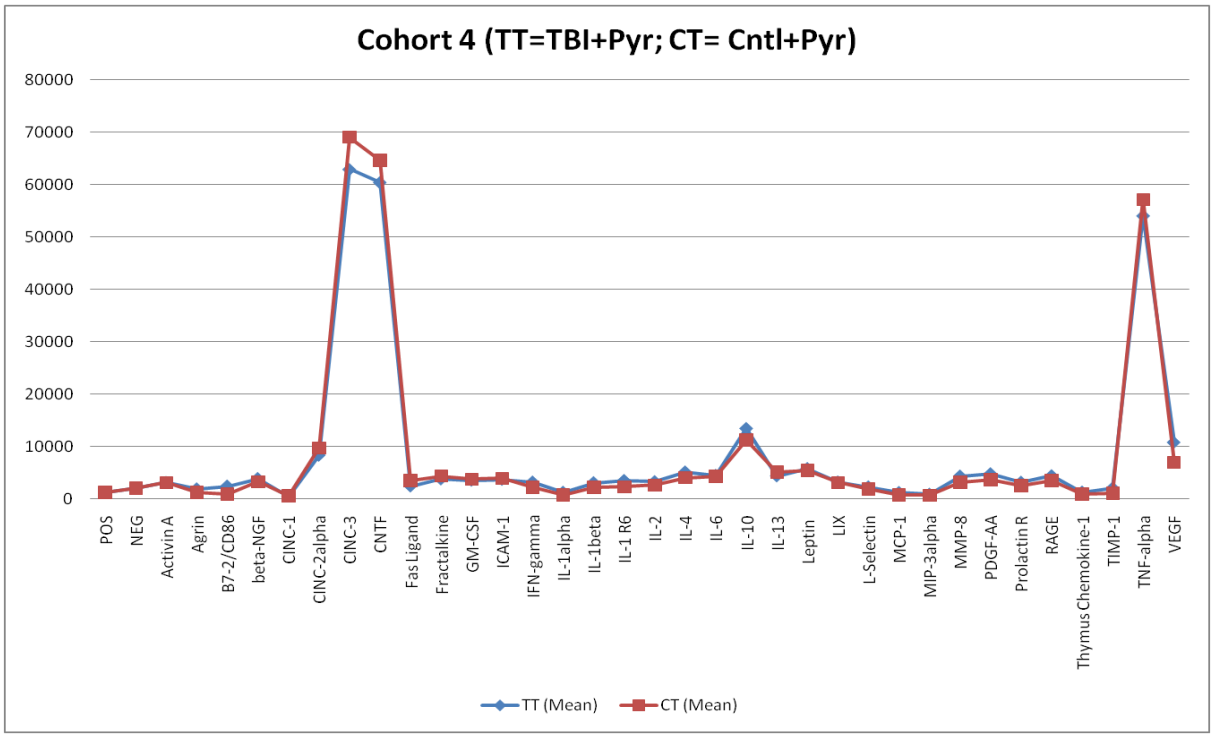

Fig. 39. General Trend of Expression Profile of Cytokines in RatHippocampus: Control is from five rats and TBI from seven rats.

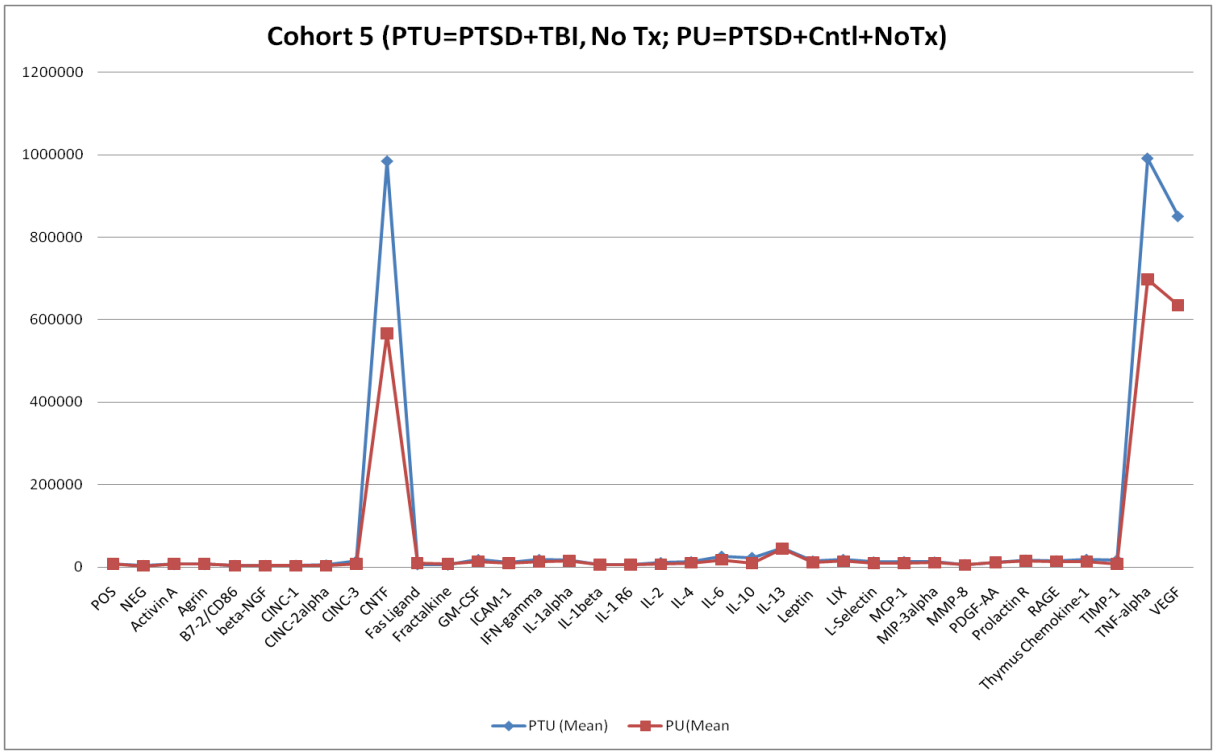

Fig. 40. General Trend of Expression Profile of Cytokines in RatHippocampus from animals subjected to PTSD, TBI+PTSD. M± SE from seven rats.

9. Key Research Accomplishments:

a. Reduced serum glucose, high base excess and increased CPK in TBI indicated compromised cellular substrate and oxygen metabolism in injured brain cells.

b. Dipstick test and PDH- Compared to controls, mitochondrial enzyme PDH measured by dipstick test was significantly increased in both blood and brain of all injured (TBI with or without PTSD) rats. There was a strong correlation between the PDH contents in blood and hippocampus, suggesting that there is possibility of a mitochondrial- targeted enzyme as a biomarker of brain injury severity. Note: *more samples are to be analyze and the work is still under progress.*

c. Dipstick test and complex I- A significant correlation between complex I in blood and hippocampus of animals with long term PTSD was noted. This relationship was not found in any other gp. of animals studied.

d. Genetic analysis of mitochondrial- targeted genes in hippocampus of TBI rats confirmed the dysregulation of genes responsible for PDH and ETC enzyme activities, as well as for several neurodegenerative disorders.

e. Altered neurobehavioral tests related to anxiety were only found in PTSD, while tests of physical strength and memory were distorted in TBI.

f. Pyruvate increased the spatial memory in TBI, PTSD and PTSD+TBI animals., In this study we have discovered that besides the neuroprotective role of pyruvate, it can also cause muscle damage because neurobehavioral test of grip strength was poor in rats treated pyruvate in both controls and TBI groups.

g. *Immunohistochemical analysis shows the adaptive mechanisms for the healing of TBI* i.e. increased GFAP, increased NEUN to stimulate the growth of neurons in the injured area, and increased mitochondrial PDH E1 in injured area confirms the repair/adaptive metabolic process in mitochondria.Certain proteins, which are known to cause secondary cell injury are also increased in TBI animals. These proteins are Tau, nitrotyrosine and myline basic protein. Our future studies will focus on identifying the therapeutic strategies to prevent the expression of these harmful proteins.

10. Reportable Outcomes:

Overall, these results suggest that even one week after TBI, the metabolic, neurobehavioral parameters and expression of cellular proteins were altered. However, the patterns of these changes were different in TBI, PTSD and PTSD+TBI. Pyruvate treatment showed neuroprotective propertives inspite of muscle damage. Blood base dipstick test of PDH enzyme as a biomarker of mitochondrial damage showed a good correlation between blood and hippocampus.

11. Conclusions:

Blood base dipstick test of PDH enzyme as a biomarker of mitochondrial damage showed a good correlation between blood and hippocampus. These results were also confirmed by mitochondrial- targeted genes in injured hippocampus.

12. Future Plans:

a. Develop more dipsticks to measure other neuro proteins such as GFAP, MABP, NEUN and Tau

b. Apply for more funding to see if blood based dipstick test of mitochondrial damage as a biomarker of brain injury severity can be used in <u>human patients with TBI and or PTSD and brain injury severity.</u>

c. Identify a combination of therapeutic strategies to treat patients with TBI, PTSD and PTSD+TBI

13. References:

1. Cernak I, Wang Z, Jiang J, Bian X, Savic J. Ultrastructural and functional characteristics of blast injury-induced neurotrauma. J Trauma. 2001;50:695-706.
2. Chen QY, Chen Q, Feng GY, Lindpaintner K, Chen Y, Sun X, Chen Z, Gao Z, Tang J, He L. Case-control association study of the close homologue of L1 (CHL1) gene and schizophrenia in the Chinese population. Schizophr Res. 2005;73:269-74.
3. Su YA, Wu J, Zhang L, Zhang Q, Su DM, He P, Wang BD, Li H, Webster MJ, Rennert OM, Ursano RJ. Dysregulated mitochondrial genes and networks with drug targets in postmortem brain of patients with posttraumatic stress disorder (PTSD) revealed by human mitochondria-focused cDNA microarrays. Int J Biol Sci. 2008;4:223-35.
4. Hoge CW, Castro CA, Messer SC, McGurk D, Cotting DI, Koffman RL. Combat duty in Iraq and Afghanistan, mental health problems, and barriers to care. N Engl J Med. 2004;351:13-22.
5. Hoge CW, Terhakopian A, Castro CA, Messer SC, Engel CC. Association of posttraumatic stress disorder with somatic symptoms, health care visits, and absenteeism among Iraq war veterans. Am J Psychiatry. 2007;164:150-3.
6. Ng K, Mikulis DJ, Glazer J, Kabani N, Till C, Greenberg G, Thompson A, Lazinski D, Agid R, Colella B, Green RE. Magnetic resonance imaging evidence of progression of subacute brain atrophy in moderate to severe traumatic brain injury. Arch Phys Med Rehabil. 2008;89:S35-44.
7. Villarreal G, King CY. Brain imaging in posttraumatic stress disorder. Semin Clin Neuropsychiatry. 2001;6:131-45.
8. Villalba M, Martinez-Serrano A, Gomez-Puertas P, Blanco P, Borner C, Villa A, Casado M, Gimenez C, Pereira R, Bogonez E, et al. The role of pyruvate in neuronal calcium homeostasis. Effects on intracellular calcium pools. J Biol Chem. 1994;269:2468-76.
9. Mongan PD, Capacchione J, Fontana JL, West S, Bunger R. Pyruvate improves cerebral metabolism during hemorrhagic shock. Am J Physiol Heart Circ Physiol. 2001;281:H854-64.
10. Moro N, Ghavim SS, Hovda DA, Sutton RL. Delayed sodium pyruvate treatment improves working memory following experimental traumatic brain injury. Neurosci Lett. 2011;491:158-62.
11. Sharma P, Benford B, Li ZZ, Ling GS. Role of pyruvate dehydrogenase complex in traumatic brain injury and Measurement of pyruvate dehydrogenase enzyme by dipstick test. J Emerg Trauma Shock. 2009;2:67-72.
12. Sharma P, Karian J, Sharma S, Liu S, Mongan PD. Pyruvate ameliorates post ischemic injury of rat astrocytes and protects them against PARP mediated cell death. Brain Res. 2003;992:104-13.
13. Bai X, Wu J, Zhang Q, Alesci S, Manoli I, Blackman MR, Chrousos GP, Goldstein AL, Rennert OM, Su YA. Third-generation human mitochondria-focused cDNA microarray and its bioinformatic tools for analysis of gene expression. Biotechniques. 2007;42:365-75.
14. Su YA, Zhang Q, Su DM, Tang MX. Rat mitochondrion-neuron focused microarray (rMNChip) and bioinformatics tools for rapid identification of differential pathways in brain tissues. Int J Biol Sci. 2011;7:308-22.
15. McIntosh TK, Vink R, Noble L, Yamakami I, Fernyak S, Soares H, *et al*.

Traumatic brain injury in the rat: Characterization of a lateral fluidpercussion model. Neuroscience 1989;28:233-44.

16. Ling GS, Lee EY, Kalehua AN. Traumatic brain injury in the rat using the fluid-percussion model. *Curr Protoc Neurosci.* 2004;9:92.

14. Appendices:

1. Abstract presented in "Neurotrauma Spectrum Conference" 2012 at NIH Bethesda
2. Publication in International J. Critical Care and Injury

13.Appendices.

1. Abstract presented in “Neurotrauma Spectrum Conference” 2012 at NIH Bethesda
2. Publication in International J. Critical Care and Injury

IJCIIS_82_12R6

Original Article

Access this article online
Website: www.ijciis.org
DOI: ***
Quick Response Code:

Mitochondrial targeted neuron focused genes in hippocampus of rats with traumatic brain injury

Pushpa Sharma, Yan A Su[1], Erin S Barry[2], Neil E Grunberg[2], Zhang Lei[3]

Department of Anesthesiology, Uniformed Services University of the Health Sciences, [1]Department of Gene and Protein Biomarkers, GenPro Markers, Inc, Rockville, Maryland, [2]Department of Medical and Clinical Psychology, [3]Department of Psychiatry, Center for the Study of Traumatic Stress, Uniformed Services University of the Health Sciences, Bethesda, MD, USA

Address for correspondence:
Dr. Pushpa Sharma,
Department of Anesthesiology, Uniformed Services University of the Health Sciences,
Bethesda, MD 20814, USA.
E-mail: psharma@usuhs.edu

ABSTRACT

Context: Mild traumatic brain injury (mTBI) represents a major health problem in civilian populations as well as among the military service members due to (1) lack of effective treatments, and (2) our incomplete understanding about the progression of secondary cell injury cascades resulting in neuronal cell death due to deficient cellular energy metabolism and damaged mitochondria.

Aims: The aim of this study was to identify and delineate the mitochondrial targeted genes responsible for altered brain energy metabolism in the injured brain.

Settings and Design: Rats were either grouped into naïve controls or received lateral fluid percussion brain injury (2–2.5 atm) and followed up for 7 days.

Materials and Methods: Rats were either grouped into naïve controls or received lateral fluid percussion brain injury (2–2.5 atm) and followed for 7 days. The severity of brain injury was evaluated by the neurological severity scale—revised (NSS-R) at 3 and 5 days post TBI and immunohistochemical analyses at 7 days post TBI. The expression profiles of mitochondrial-targeted genes across the hippocampus from TBI and naïve rats were also examined by oligo-DNA microarrays.

Results: NSS-R scores of TBI rats (5.4 ± 0.5) in comparison to naïve rats (3.9 ± 0.5) and H and E staining of brain sections suggested a mild brain injury. Bioinformatics and systems biology analyses showed 31 dysregulated genes, 10 affected canonical molecular pathways including a number of genes involved in mitochondrial enzymes for oxidative phosphorylation, mitogen-activated protein Kinase (MAP), peroxisome proliferator-activated protein (PPAP), apoptosis signaling, and genes responsible for long-term potentiation of Alzheimer's and Parkinson's diseases.

Conclusions: Our results suggest that dysregulated mitochondrial-focused genes in injured brains may have a clinical utility for the development of future therapeutic strategies aimed at the treatment of TBI.

Key Words: Brain trauma, fluid percussion, gene expression, hippocampus, mitochondria, neurological severity scale

INTRODUCTION

Traumatic brain injury (TBI) has recently been recognized as the silent, signature wound of the wars in Iraq and Afghanistan.[1] From 2000 to 2010, approximately 1.6 million service members have been deployed to date in Iraq and Afghanistan. During this time period almost 179,000 service members sustained a TBI with the vast majority, about 137,000 of those being classified as mild in terms of severity.[2] In the United States, TBIs are also common in the civilian population, with an estimated 1.7 million civilians sustaining a mild to moderate TBI annually where approximately 75% of these injuries are classified as mild TBI (mTBI).[3] Therefore, even a slight improvement in the diagnostic and neuroprotective strategies will have significant health implications.

The mild–moderate closed head trauma is initiated by the impact of the brain against the inner side of the calvarium. Subsequently, there begins a series of complex biochemical, cellular, metabolic, and physiological injury cascade that may take longer to complete complete.[4,5] These mild–moderate brain injuries are invisible from the outside, but the cognitive deficits, including memory impairment, are common neurological consequences of TBI and the underlying mechanisms are poorly defined.[6] The hippocampus is one of the key regions of the brain responsible for learning and long-term memories. Both clinical and experimental evidence suggest that long-term effects of mTBI cause hippocampal neuronal cell death, which is associated with cognitive impairment.[7] Lateral fluid percussion injury (FPI) in rodents replicates several clinically relevant features of human TBI. It has been widely used in the investigation of biochemical and pathological responses observed in human closed head injuries.[8]

The growing evidence suggests the important role of mitochondria in the progression of TBI and a subcellular target for neuroprotective strategies.[9] Following TBI, excessive release of the neurotransmitter glutamate can result in mitochondrial dysfunctions by causing a toxic influx of calcium into brain cells. Mitochondrion has its own DNA (mtDNA), which encodes only 37 genes: 13 for various subunits of electron transport chain complexes I, II, III, IV, and V; 22 mt genes for mitochondrial tRNA and remaining 2 genes encodes rRNA. Most mitochondrial proteins including those for electron transport chain enzymes to produce cellular ATP, cell signaling, and apoptosis are encoded and/or regulated by nuclear DNA. In comparison to nuclear DNA, mtDNA is very sensitive to oxidative damage due to lack of histones.[10-16] Therefore, any damage to mtDNA will have grave consequences on the depletion of cellular ATP, increase free radicals, DNA damage, and neuronal cell death, which is observed in clinical and experimental TBI.[1,9] To our knowledge, neuronal-targeted expression profiles of mitochondria-focused genes have not been examined as a potential therapeutic target for mTBI. To date, methods employing a systems biology approach to identify the mitochondria-focused genes in the hippocampus underlying the pathogenesis of TBI have also not been documented.

In this study, we have examined the neurobehavioral and histochemical response to the brain injury, and analyzed the mitochondria-focused oligo-DNA microarray to determine the expression profile of mitochondria-focused genes in the hippocampus of rats with TBI induced by lateral fluid percussion injury.

MATERIALS AND METHODS

Adult, male Sprague–Dawley rats (225–275 G, Harlan, Frederick, MD, USA) were pair housed in standard polycarbonate shoebox cages (42.5 × 20.5 × 20 cm) with hardwood chip bedding (Pine-Dri) in an environmentally controlled animal facility under a 12-h reverse light–dark cycle. Food (Harlan Teklad 4% Mouse/Rat Diet 7001) and water were available *ad libitum*. Rats were left to acclimate for 1 week to the vivarium before use. All procedures were performed to National Institutes of Health (NIH) guidelines and were approved by the Institutional Animal Care and Use Committee (IACUC). A total of 12 animals/group were included in this study. All animals had neurobehavioral evaluation. Hippocampi from three animals/group were used for hematoxylin and eosin stain (H and E staining) (total six animals), and three animals from each group had mitochondrial genetic profile mapped (total six animals). Remaining tissues were stored for further analysis.

Instrumentation and induction of fluid percussion injury

Mild injury was induced in rats according to our published procedure.[17] In brief, animals were anesthetized with 1–3% isoflourane in oxygen. Under sterile conditions, a 3 cm sagittal incision was made along the midline to expose the cranium. A 5 mm burr hole was placed 2 mm to the right of the sagittal suture halfway between bregma and lamda using a 5 mm trephine drill bit exposing the dura. A Luer-Loc needle hub was placed into the burr hole and cemented to the cranium using cyanoacrilate. The glue was allowed to completely dry, and the empty Luer-Loc hub was filled with normal saline before being connected to the TBI device. A fluid percussion pulse of 2.0–2.5 atm was administered by an injury cannula positioned parasagittally over the right cerebral cortex. The fluid percussion pulse was administered by a pendulum modulated fluid percussion biomechanical device (Richmond, VA, USA), the Luer-Loc hub was removed and defects in the cranium were repaired with bone wax. The skin was then closed with a surgical skin stapler. Animals were allowed to stabilize in the warm blanket and then returned to their cages and moved to the animal facility at the Uniformed Services University of the Health Sciences. At 7 days post TBI, animals were anesthetized, and brains were removed followed by the dissection of hippocampus. Hippocampi were dissected according to the method described by Jacobowitz and modified by Hefner *et al*.[18,19] The consistency of the hippocampus region of the brain was confirmed by measuring the regional specific protein levels, which were in the range of 10.8–11.2 mg/ml in all the animals examined. Simultaneously, animals in the naïve control group were also housed in the same environmental conditions. These naïve animals were time matched and did not receive any brain injury. Seven days postinjury (day 7), TBI and naïve animals were sacrificed. The hippocampi from the right side of the brain of three animals per group were used for RNA isolation and subsequent gene profiling.

Animal behavioral measures

Behavior was observed during the animals' dark cycle. Behaviors were measured prior to injury (baseline) and at two time points during the week after injury (3 days post TBI = T1; 5 days post TBI = T2). Behavioral measures included the neurological severity scale—revised (NSS-R) to measure neurobehavioral responses. The NSS-R is a series of 10 specific behavioral measures[20] based on several neurological severity scales (NSS) designed for rats.[21-24] The NSS-R measures motor, sensory, and reflex responses. The NSS-R was scored by an experienced rater who was previously trained until reaching high inter-rater reliability with other independent raters. Each response was scored from 0–2, where 0 = normal response, 1 = partial and/or compromised impairment, and 2 = lack of ability to perform the task. A composite score was calculated (0–20), where the higher the score indicates more neurobehavioral impairment. The testing was conducted using two empty polycarbonate cages (46 × 36 × 20 cm) with no bedding or lid. The equipment was cleaned between each animal.

Immunohistochemistry

One week postinjury, a subset of three animals per group were subjected to formalin perfusion and immunohistochemistry as described previously.[17] Briefly, rats were deeply anesthetized with isoflurane inhalational anesthesia perfused transcardially with 400 ml of 4% fresh depolymerized paraformaldehyde in phosphate buffered saline (Fisher Scientific) using a peristaltic pump at a flow rate of approximately 60–80 ml/min. Brains were carefully dissected, and postfixed in 4% paraformaldehyde for 1 day. The tissues were cryoprotected by sequential passage through 10%, 20%, and 30% sucrose in phosphate buffered solution (PBS) for 1 day each. Tissues were kept in 30% sucrose at 4°C until used. The brains were rapidly frozen and 10–20 μm coronal sections were cut in a cryostat set at a temperature of-20°C. Sections collected on treated slides were stained with H and E to determine a broad range of cytoplasmic, nuclear, and extracellular matrix features. Hematoxylin has a deep blue-purple color and stains nucleic acids, while eosin is pink and stains proteins nonspecifically. In a typical tissue, nuclei are stained blue, whereas the cytoplasm and extracellular matrix have varying degrees of pink staining.

RMNchip

High quality rat mitochondrion-neuron focused microarrays (rMNChip) were designed and fabricated as described previously.[15] Briefly, rMNChip contains 1,500 genes including 37 mitochondrial DNA (mtDNA)-encoded genes, 1,098 nuclear DNA (nDNA)-encoded and mitochondria-focused genes, and 365 neuron-related genes. The oligonucleotides for genes and positive (80 housekeeping genes) and negative (no rat DNA) controls on rMNChip were printed, each in triplicates, onto the N-hydroxysuccinimide ester reactive groups-coated glass slides. rMNChip microarrays were fabricated in the Class 100 super-clean environment as described previously.[15]

RNA isolation and purification

Each sample of total RNA was purified from hippocampi collected in a RNA tube and processed using the RNA Kit (PAXgene RNA Kit, 762164, QIAGEN, USA) following the manufacturer's instructions.

Microarray hybridization

One microgram RNA per sample was used for Cy5-dUTP labeling of cDNA by use of the express array detection kit (3DNA Array 900, Genisphere, Hatfield, PA, USA) following the manufacturer's instructions. Slides were scanned using 5 micron resolution and LOWESS method with Scan Array Microarray Scanner (PerkinElmer). Triplicate microarray experiments were performed for each and every RNA sample. Thus, the RNA level of each and every gene was measured as many as nine times. The background-subtracted mean values of the measurements were used for microarray data analysis. All microarray experiments were performed in the same laboratory of Gen Pro Markers, Inc.[15]

Microarray database, bioinformatics and systems biology

Gene expression database was constructed using FileMaker software (FileMaker Pro, Inc., Santa Clara, CA, USA). Database construction, data filtering, and selection were performed as described previously.[10,15] The quantile normalization method[25] in software R version 2.7.1 (the R Foundation for Statistical Computing) was used to normalize microarray data. The normalized data was used to cluster and visualize genes and hippocampus tissue samples by using software Cluster version 3.0 and the resulting heat map was visualized by using MapleTree software (http://rana.lbl.gov/EisenSoftware.htm). Gene information including identification numbers, official symbols and full names were updated using the National Center for Biotechnology Information (NCBI) database (www.ncbi.nlm.nih.gov/gene). Kyoto Encyclopedia of Genes and Genomes (KEGG) pathways were computed using DAVID Bioinformatics Resources (http://david.abcc.ncifcrf.gov).

Statistics

The quantile normalization method in software R/Bioconductor version 2.7.1 (The R Foundation for Statistical Computing) was used to normalize data. Statistical calculations were performed on triplicate spots per gene and triplicate array experiments using XLSTAT 2006 (XLSTAT, New York, NY, USA). The moderated *P*-values and false discovery rate (FDR) for multiple statistical testing with Benjamini and Hochberg methods were calculated with DAVID Bioinformatics Resources version 6.7 (http://david.abcc.ncifcrf.gov). Differentially expressed genes were identified arbitrarily by ≥1.4-fold

change in the average expression of the background-subtracted mean intensity ratios of a gene between TBI and naïve rats, with *P*-value < 0.05. Repeated measures analysis of variance (rANOVA) were conducted for the NSS-R (N = 24). All tests were two tailed using alpha = 0.05.

RESULTS

Effects of TBI on neurological severity scale - revised

Figure 1 presents the NSS-R scores. There were no differences in NSS-R scores between experimental groups at baseline. Post TBI, the TBI rats (5.58 ± 0.48) had significantly greater NSS-R scores compared with the naïve rats (3.92 ± 0.48), $F(1, 22) = 5.93$, $P = 0.023$, $\eta^2 = 0.212$. Additionally, the TBI rats (5.42 ± 0.50) had significantly greater scores than the naïve rats (3.25 ± 0.50) at T2, $F(1, 22) = 9.23$, $P = 0.006$, $\eta^2 = 0.295$. This finding suggests that TBI rats suffered more neurological impairment than the naïve rats.

Hematoxylin and eosin staining

Figure 2 depicts the H and E immunosatined brain section from TBI and naïve rats. In comparison to naïve rats [Figure 2a], the injured brain section [Figure 2b] is showing the hippocampal commissure, which is the anterior part of the white matter of the hippocampus, and is inverted v shaped fiber bundle at the center of the tissue. Obvious histological injury is only on the cortex, which is at the right upper part of the 'TBI' section on the cortex. A breach in the surface of the cortex and an increase in hematoxylin stained (blue) nuclei 'newer' cells in the lesion suggest a minor injury on the surface and possibly the healing process through the generation of new cells.

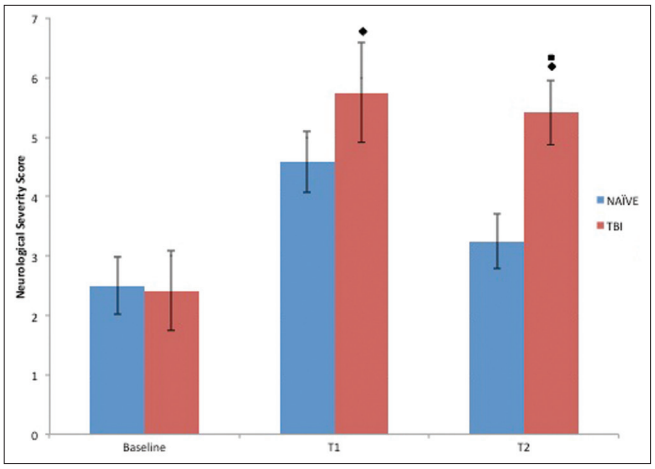

Figure 1: Effect of TBI on neurological severity score–revised (NSS-R): Neurological severity is determined using a 10-item test with a score of 0, 1, or 2, given on each task. A greater score for a rat indicates more neurobehavioral impairment. All animals were evaluated at baseline (BL), day 3 (T1) and day 5 (T2) postinjury. Time matched naïve animals were also evaluated at BL, T1 and T2 time period. ■ $P < 0.05$, naïve compared with TBI at T2, ♦ $P < 0.05$, differed from BL (either T1 or T2)

Expression levels of 1,448 of 1,500 mitochondrion-neuron focused genes are informative

Expression clusters of mitochondria-focused genes were obtained from both TBI and naïve groups of animals. Total RNA samples were extracted from the hippocampus of rats with or without TBI and labeled for triplicate microarray experiments using our recently developed rMNChip. To avoid misclassification, each of 1,500 genes on rMNChip was measured nine times (three identical probes per microarray and three microarray experiments per specimen), which generated reliable expression data for further analysis. The microarray data of spots across all gene chips used for RNA samples were filtered by uniform statistic and bioinformatic criteria described previously,[10] which generated 1,448 genes with informative expression data. Figure 3 shows the box plots of RNA levels of 1,448 genes before and after the data normalization. The normalized data were used for unsupervised clustering analysis and identification of differentially expressed genes.

Expression patterns of 235 and 105 genes in hippocampus differentiate mTBI from naïve rats

By using ≥1.25-fold change in the average expression of the background-subtracted mean intensity ratios of a gene between TBI and naïve as criteria, 235 of 1,448 informative genes in the hippocampus are able to differentiate mTBI from the naïve rats based on the unsupervised cluster analysis [Figure 4a and b]. By increasing the stringency to ≥1.60-fold changes, the patterns of 105 genes differentiate mTBI from the naïve rats with much clear cluster results [Figure 4c].

Identification of 10 canonical molecular pathways with a significant number of dysregulated genes

By applying differentially expressed genes to the NCBI DAVID Bioinformatics Resources, we identified 10 canonical molecular pathways including Alzheimer's disease, mitogen-activated protein kinase (MAPK) signaling, Parkinson's disease, apoptosis, oxidative

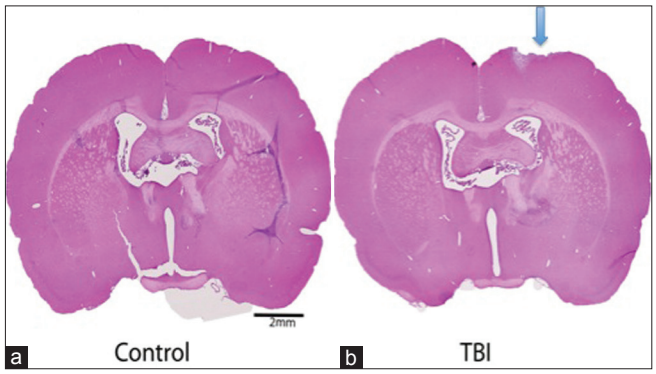

Figure 2: (a,b) Histochemical examination of TBI: Comparison of hematoxylin and eosin staining in brain sections obtained from naïve and post TBI. In comparison to naïve, the histological injury is only seen as a breach in the surface of the cortex, which is at the right upper part of the TBI

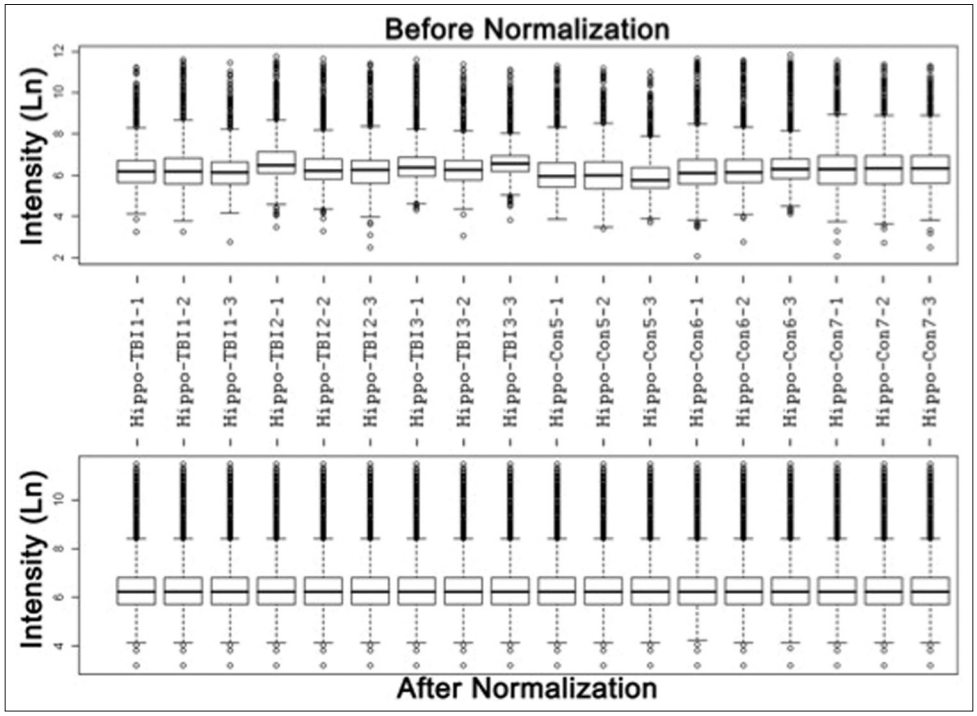

Figure 3: Box plots of expression data before and after normalization: The quantile normalization algorithms were used to adjust the values of the background-subtracted mean pixel intensities of triplicate measurements per microarray for each and every set of 1,500 genes. The expression levels of each of 1,500 genes in most of these hippocampus samples of six rats with or without TBI were measured by microarray experiments with both technical triplicates and experimental triplicates. In contrast to the prenormalization boxplots (top panel), the postnormalized box plots distribute in the same intervals with the same density center, indicating successful adjustment of data. The postnormalized data were used for further analysis

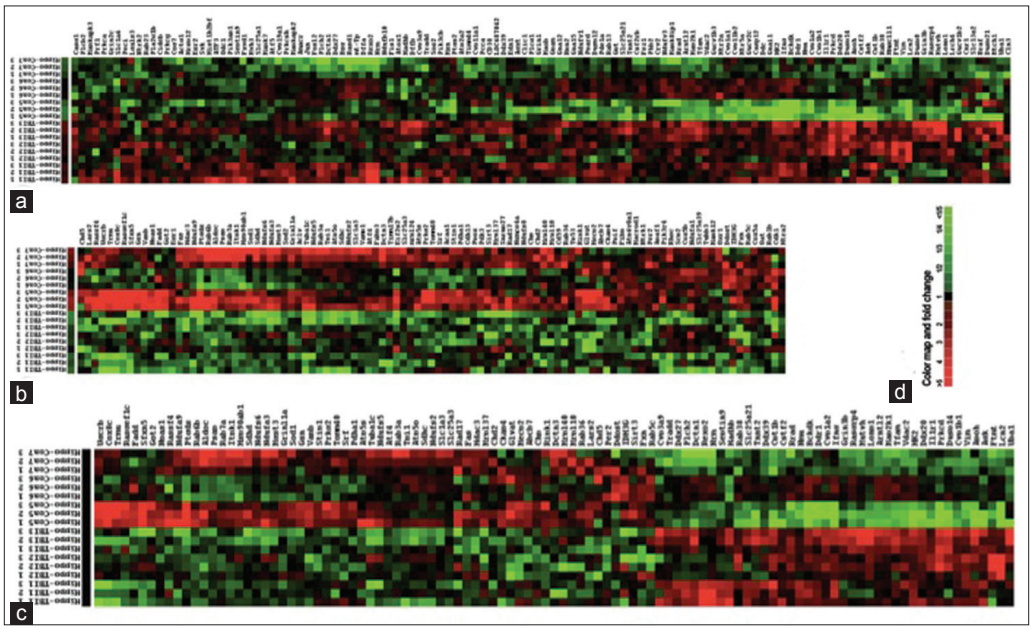

Figure 4: Dendrogram and heat maps of 235 gene expression in hippocampus of rat model of traumatic brain injury (TBI) and naïve. The dendrogram of unsupervised cluster of three TBI and three naïve (a) and (b) based on expression similarities of 235 rat mitochondria-neuron genes. (c) The dendrogram of upsupervised cluster of the same samples based on expression similarities of 105 genes. These heat maps classifies the hippocampus tissue samples into two groups. (d) Color map and fold changes indicated. Green: Down-regulation; red: Up-regulation; black: No change

phosphorylation, Huntington's disease, amyotrophic lateral sclerosis, long-term potentiation, peroxisome proliferator-activated receptors (PPARs) signaling, and vascular endothelial growth factor (VEGF) signaling pathways [Table 1].

DISCUSSION

The aim of this translational study was to examine the expression profiling of mitochondria-focused genes in the hippocampus of a rodent TBI model: To identify the

Table 1: Pathways with a significant number of dysregulated genes in rat traumatic brain injury hippocampus

KEGG_Pathway	Genes	Count	%	*P* Value	Benjamini
Alzheimer's disease	Ndufs2, Atp5o, Fas, Cox5b, Apaf1, Chp	6	17.1	1.30E-03	7.90E-02
MAPK signaling pathway	Mapk12, Fas, Prkcg, Chp, Atf4, Ntrk1	6	17.1	4.70E-03	9.80E-02
Parkinson's disease	Ndufs2, Atp5o, Htra2, Cox5b, Apaf1	5	14.3	2.90E-03	8.90E-02
Apoptosis	Fas, Apaf1, Chp, Ntrk1	4	11.4	5.50E-03	8.50E-02
Oxidative phosphorylation	Atp6v0a1, Ndufs2, Atp5o, Cox5b	4	11.4	2.00E-02	2.30E-01
Huntington's disease	Ndufs2, Atp5o, Cox5b, Apaf1	4	11.4	4.60E-02	2.70E-01
Amyotrophic lateral sclerosis	Mapk12, Apaf1, Chp	3	8.6	2.60E-02	2.50E-01
Long-term potentiation	Prkcg, Chp, Atf4	3	8.6	3.30E-02	2.70E-01
PPAR signaling pathway	Fabp3, Cpt1b, Scp2	3	8.6	3.70E-02	2.60E-01
VEGF signaling pathway	Mapk12, Prkcg, Chp	3	8.6	4.00E-02	2.50E-01

Analysis of significantly dysregulated genes in the hippocampus of TBI rats suggest that several pathways responsible for mitochondrial metabolic derangements, cell signaling and apoptosis were affected when compared with control animals. These dysregulated genes in TBI were also found to be associated with certain neurodegenerative disorders

gene clusters, the pathways related to either diseases or to related signal transduction pathways. These pathways are indicated as possible therapeutic targets for TBI. In this study we also searched for changes at individual gene expression level, which potentially may serve as a therapeutic target for the treatment of TBI and associated neurodegenerative diseases.

The rat model of lateral fluid percussion injury is one of the most accepted animal model to replicate human TBI in terms of biochemical and metabolic pathways.[26] However, in this rat model, it is difficult to diagnose the severity of brain injury because animals are anesthetized at the time of injury. Therefore, the level of consciousness cannot be used as the measurement of brain injury severity. However, we have compared the NSS-R scores prior to injury and then 3 and 5 days post TBI. Baseline scores were similar between groups, but by 3 and 5 days post TBI, the TBI animals had almost a 2-fold increase in their NSS-R score that remained elevated over both time points. This suggests an impaired neurobehavioral function similar to mild-moderate TBI in humans. Our H and E stained brain sections did not show any gross and/or histological damage in the hippocampus except a slight tissue distortion at the point of impact suggesting a mild TBI. FPI induces both focal and diffuse axonal injury, which often results in the failure of cellular metabolism and neuronal cell death. Therefore, we have compared the neuronal focused mitochondrial genes in the hippocampus of injured and naïve animals due to its key role in cognitive functions.

The advent of high-throughput genomics, such as gene microarrays, has led to an unprecedented surge of cross-disciplinary work between biology and statistics. However, quality assessment of microarray data is an important and often challenging aspect of gene expression analysis. The application of machine-learning techniques (also known as pattern-recognition techniques) to large biological data sets has been used to identify groups of functionally related genes,[11] to predict broader biological phenotypes and genetic interactions,[27] and to diagnosis post-traumatic stress disorder (PTSD).[14] Since the algorithmic basis of clustering, the application of unsupervised machine-learning techniques to identify the patterns inherent in a data set, is well established, we have used this approach in this current study. Unsupervised techniques are exploratory. It lets the data organize itself, and then we try to find biological meaning. This approach is to understand whole data and produce a visualization of the data. Briefly, like the methods used in other research areas, we first quantified the scanned image into numeric data amenable to statistical analysis. We filtered the raw data set, all spots across all gene chips of 16 rats (TBI and naïve) by removing the high-noise and low-signal spots. After that, we normalized the data to remove spatial variability, channel imbalances and inter array heterogeneity [Figure 3]. Then, we were able to use the cluster approaches to identify broad patterns. Using this approach we were able to produce a visualization of the data, hierarchical clustering. Our hierarchical clustering generated dendrograms demonstrated up- and downregulated gene clusters in all rats, including TBI and naïve [Figure 4]. These unsupervised analysis data indicated grouping of genes having similar expression patterns or clustering. The approaches are based on the assumption that the whole set of microarray data is a finite mixture of a certain type of distributions with different parameters. Application of the model-based algorithms to unsupervised clustering has been reported in PTSD study.[14] We hypothesize that unknown gene X is similar in expression to known genes A and B, or they are involved in the same/related pathway.

In a complex disorder such as mTBI, clustering a variety of risk factors can improve predictive value. Integrative biomarkers can be developed through superposition of mRNA. Clustering can prioritize functionally plausible candidate genes. Clustering aggregates information from multiple loci into association scores for pathways[28] and informs drug development by predicting therapeutic gene targets. Clustering can also identify pathways affected by an existing drug, either to predict the mode of action or suggest drug repurposing in which drugs developed for known disorders can serve as a new compound for TBI. Based on the unsupervised cluster results,

10 networks of dysregulated genes involved in neuron function and neurological disorders were identified and presented in Table 1. These pathways are involved in several networks related to neuronal disorders, such as Alzheimer's, Huntington, and Parkinson's diseases. Our results also provide an important direction to monitor the TBI patients for these neurodegenerative disorders as a consequence of delayed traumatic brain injury due to progressive mitochondrial damage.[4,7,29]

In addition to the identification of mitochondrial genes for the neurodegenerative disorders, we have also documented several genes responsible for altered metabolic pathways, signaling and apoptotic pathways in TBI rats compared with naïve animals. Therefore, an orchestrated mitochondrial genes network and pathways mechanisms identified in TBI [Table 1] may also serve as future blood-based mitogenetic biomarkers for TBI.

Limitations of the study

The data obtained from three samples in each group is the bare minimum number allowing calculation of standard deviation and statistical significant difference permitting the comparison between TBI and control group. Although a larger sample size would strengthen this paper significantly, this small sample size is also the starting point for a pilot study to determine the reliability and validity of our mitochondrial focused gene-profiling data in response to TBI. This study will also allow us to estimate the sample size for a larger-scale study.

In this study, we have used naïve animals without craniotomy or anesthesia as control group. Our study also raises the question of the appropriate use of control animals for TBI induced by FPI that requires the craniotomy. In a recent study by Cole *et al*. (2011), craniotomy alone results in traumatic brain injury with morphological, biochemical, and behavioral correlates.[30] In addition, the significantly increased expression in cytokines after craniotomy alone can initiate numerous secondary cascades similar to the posttraumatic changes in brain physiology. Therefore, due to the diverse nature of injury caused by craniotomy procedures, it may be ben eficial to avoid this procedure as a control group and use naïve animals as controls.

CONCLUSION

Our data suggest that mitochondria-mediated cellular and molecular response to TBI is essential for the cell survival and in prevention of long-term neurodegenerative disorders associated with brain injury. Our findings also suggest that mitochondria-focused and TBI-responsive genes may play a key role in the pathogenesis of TBI. Meanwhile, the identification and validation of the dysregulated genes enhances our understanding of the cellular and molecular mechanisms underlying the pathophysiology of TBI. We expect more studies to test the clinical utility of mitochondria-focused genes as therapeutic targets for the treatment of TBI.

Analysis of significantly dysregulated genes in the hippocampus of TBI rats suggest that several pathways responsible for mitochondrial metabolic derangements, cell signaling and apoptosis were affected when compared with control animals. These dysregulated genes in TBI were also found to be associated with certain neurodegenerative disorders.

ACKNOWLEDGEMENT

We thank Dr. Xianzhang Hu and Dr. Xiaoxia Li for RNA isolation and purification. Dr. Fei Meng and Mr. Michael Tang for their services of microarray contract, and Mrs. Brandi Benford for her excellent surgical skills in performing TBI.

REFERENCES

1. Hoge CW, Castro CA, Messer SC, McGurk D, Cotting DI, Koffman RL. Combat duty in Iraq and Afghanistan, mental health problems, and barriers to care. N Engl J Med 2004;351:13-22.
2. Warden D. Military TBI during the Iraq and Afghanistan wars. J Head Trauma Rehabil 2006;21:398-402.
3. Center for Disease Control, NIH. Traumatic Brain Injury in the United States: A Report to Congress. 2001.
4. Giza CC, Hovda DA. The neurometabolic cascade of concussion. J Athl Train 2001;36:228-35.
5. Verweij BH, Muizelaar JP, Vinas FC, Peterson PL, Xiong Y, Lee CP. Impaired cerebral mitochondrial function after traumatic brain injury in humans. J Neurosurg 2000;93:815-20.
6. Sanders MJ, Sick TJ, Perez-Pinzon MA, Dietrich WD, Green EJ. Chronic failure in the maintenance of long-term potentiation following fluid percussion injury in the rat. Brain Res 2000;861:69-76.
7. Royo NC, Conte V, Saatman KE, Shimizu S, Belfield CM, Soltesz KM, *et al*. Hippocampal vulnerability following traumatic brain injury: A potential role for neurotrophin-4/5 in pyramidal cell neuroprotection. Eur J Neurosci 2006;23:1089-102.
8. Thompson HJ, Lifshitz J, Marklund N, Grady MS, Graham DI, Hovda DA, *et al*. Lateral fluid percussion brain injury: A 15-year review and evaluation. J Neurotrauma 2005;22:42-75.
9. Cernak I, Wang Z, Jiang J, Bian X, Savic J. Ultrastructural and functional characteristics of blast injury-induced neurotrauma. J Trauma 2001;50:695-706.
10. Bai X, Wu J, Zhang Q, Alesci S, Manoli I, Blackman MR, *et al*. Third-generation human mitochondria-focused cDNA microarray and its bioinformatic tools for analysis of gene expression. Biotechniques 2007;42:365-75.
11. Hughes TR, Roberts CJ, Dai H, Jones AR, Meyer MR, Slade D, *et al*. Widespread aneuploidy revealed by DNA microarray expression profiling. Nat Genet 2000;25:333-7.
12. Madrigal JL, Olivenza R, Moro MA, Lizasoain I, Lorenzo P, Rodrigo J, *et al*. Glutathione depletion, lipid peroxidation and mitochondrial dysfunction are induced by chronic stress in rat brain. Neuropsychopharmacology 2001;24:420-9.
13. Manoli I, Alesci S, Blackman MR, Su YA, Rennert OM, Chrousos GP. Mitochondria as key components of the stress response. Trends Endocrinol Metab 2007;18:190-8.
14. Su YA, Wu J, Zhang L, Zhang Q, Su DM, He P, *et al*. Dysregulated mitochondrial genes and networks with drug targets in postmortem

brain of patients with posttraumatic stress disorder (PTSD) revealed by human mitochondria-focused cDNA microarrays. Int J Biol Sci 2008;4:223-35.
15. Su YA, Zhang Q, Su DM, Tang MX. Rat mitochondrion-neuron focused microarray (rMNChip) and bioinformatics tools for rapid identification of differential pathways in brain tissues. Int J Biol Sci 2011;7:308-22.
16. Zhang L, Zhou R, Li X, Ursano RJ, Li H. Stress-induced change of mitochondria membrane potential regulated by genomic and non-genomic GR signaling: A possible mechanism for hippocampus atrophy in PTSD. Med Hypotheses 2006;66:1205-8.
17. Sharma P, Benford B, Li ZZ, Ling GS. Role of pyruvate dehydrogenase complex in traumatic brain injury and Measurement of pyruvate dehydrogenase enzyme by dipstick test. J Emerg Trauma Shock 2009;2:67-72.
18. Heffner TG, Hartman JA, Seiden LS. A rapid method for the regional dissection of the rat brain. Pharmacol Biochem Behav 1980;13:453-6.
19. Jacobowitz DM. Removal of discrete fresh regions of the rat brain. Brain Res 1974;80:111-5.
20. Kamnaksh A, Kovesdi E, Kwon SK, Wingo D, Ahmed F, Grunberg NE, *et al*. Factors affecting blast traumatic brain injury. J Neurotrauma 2011;28:2145-53.
21. Hamm RJ. Neurobehavioral assessment of outcome following traumatic brain injury in rats: An evaluation of selected measures. J Neurotrauma 2001;18:1207-16.
22. Mahmood A, Lu D, Wang L, Li Y, Lu M, Chopp M. Treatment of traumatic brain injury in female rats with intravenous administration of bone marrow stromal cells. Neurosurgery 2001;49:1196-203.
23. Marti M, Mela F, Fantin M, Zucchini S, Brown JM, Witta J, *et al*. Blockade of nociceptin/orphanin FQ transmission attenuates symptoms and neurodegeneration associated with Parkinson's disease. J Neurosci 2005;25:9591-601.
24. Shohami E, Novikov M, Bass R. Long-term effect of HU-211, a novel non-competitive NMDA antagonist, on motor and memory functions after closed head injury in the rat. Brain Res 1995;674:55-62.
25. Bolstad BM, Irizarry RA, Astrand M, Speed TP. A comparison of normalization methods for high density oligonucleotide array data based on variance and bias. Bioinformatics 2003;19:185-93.
26. McIntosh TK, Vink R, Noble L, Yamakami I, Fernyak S, Soares H, *et al*. Traumatic brain injury in the rat: Characterization of a lateral fluid-percussion model. Neuroscience 1989;28:233-44.
27. Tong AH, Lesage G, Bader GD, Ding H, Xu H, Xin X, *et al*. Global mapping of the yeast genetic interaction network. Science 2004;303:808-13.
28. Chen S, Wang C, Eberly LE, Caffo BS, Schwartz BS. Adaptive control of the false discovery rate in voxel-based morphometry. Hum Brain Mapp 2009;30:2304-11.
29. Parihar MS, Brewer GJ. Mitoenergetic failure in Alzheimer disease. Am J Physiol Cell Physiol 2007;292:C8-23.
30. Cole JT, Yarnell A, Kean WS, Gold E, Lewis B, Ren M, *et al*. Craniotomy: True sham for traumatic brain injury, or a sham of a sham? J Neurotrauma 2011;28:359-69.

Cite this article as: Citation will be included before issue gets online***

Source of Support: This study was supported by funding from DARPA to PS. Award No. W911NF-11-1-0005., **Conflict of Interest:** No.

INFLAMMATORY BIOMARKERS OF TBI/PTSD: A CORRELATIVE IMMUNO-HISTOCHEMICAL STUDY

Prasanth S. Ariyannur[1], Brandi Benford[1], David Rhoiney[1], He Li[2], Pushpa Sharma[1]

[1]Department of Anesthesiology, [2] Department of Psychiatry, Uniformed Services University of the Health Sciences, Bethesda, MD 20814

Introduction

- Acute inflammatory reaction is one of the critical mechanisms involved in the post injury patho-physiology of TBI/PTSD and its recovery.
- Biomolecules such as intra-cellular signals, structural and enzyme proteins related to cellular inflammation have been implicated as major biomarkers for TBI/PTSD.
- Peripheral biomarkers reflecting the extend of local injury and the rapidity of recovery process of pathophysiology are poorly correlated from the studies so far because of the multitude of reasons including unpredictability of barrier interruption and/ or other associated systemic non-CNS pathophysiology.

Experimental Design

Using previously described established models of TBI and PTSD, we pursue a systematic correlative study using a set of cytokine biomarkers involving CNS inflammation following an acute traumatic contusive brain injury with and with out PTSD.

Materials and Methods

Traumatic Brain Injury

Liquid percussion model of TBI was done with sufficient pre and post surgery preparations as described previously (*1*) with or with out PTSD one week prior (*2*). The animals were observed for seven days for behavioral assessments. Sodium Pyruvate treated group received Intragastric administration at a dose of 1g/kg everyday (*1*).

Tissue Preparation

The animals were sacrificed on the 7th post-TBI day and tissues were harvested. Sera was obtained from an intracardiac arterial blood draw and subsequent low speed centrifugation. The brain tissue was dissected after harvest and divided in to different parts (frontal, parietal cortices, hippocampus and brain stem cerebellum). The tissues were homogenized in lysis buffer with DTT, Nuclear pellet was spun down after low speed centrifugation. Protein was estimated prior to further studies.

Microarray

Rat Cytokine Antibody Array II (Raybio pharmaceuticals Inc.) was used. The method was exactly as described by the company. For hippocampus homogenate 200µg total protein was used.

Immunohistochemistry

Animals were perfused with neutral buffered formaldehyde and brain immunohistochemistry was done as described previously (*3*) with minor modifications in regards to the dilutions of specific primary and secondary antibodies used according to the particular tissues and imaging requirements. Images were acquired using Carl Zeiss AIM PASCAL LSCM and edited using Zeiss Image Browser and Adobe Photoshop®.

Results

Figure 1: The expression profile trend of thirty four Cytokine marker signals are shown from the sera (Top) of injured and uninjured rats is compared with that of hippocampus cytokine profile of TBI brain with out PTSD (middle) and TBI with PTSD (bottom). The results are the mean expression intensity of six rats in each of the group for TBI and Control and three animals per group for TBI ± PTSD. The mean values are shown to depict the trend. See the tabular column detailing the description of the cytokine markers and their significance. The difference in expression profile is depicted more in the tabular column.

Results

Expression Profile of Cytokines

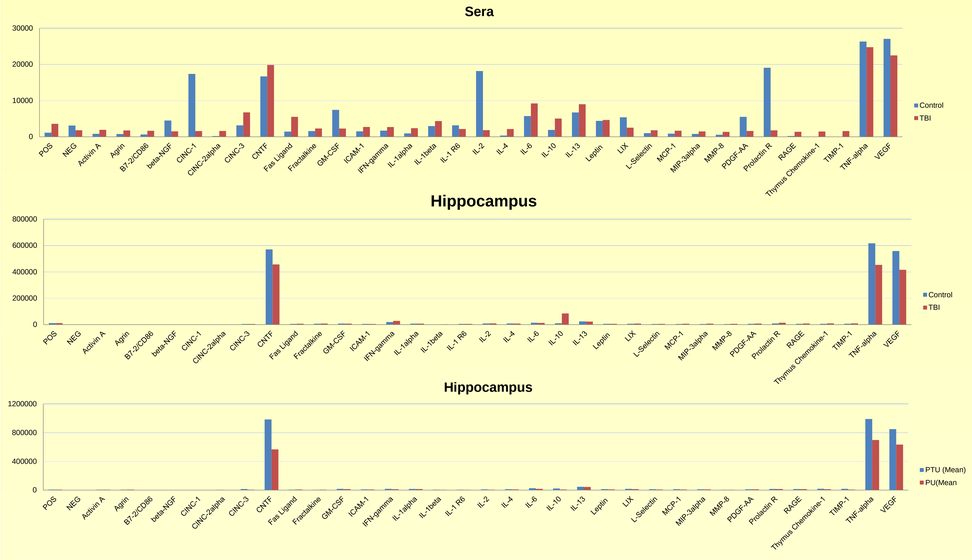

Immunohistochemistry of Peri-lesional Cortex

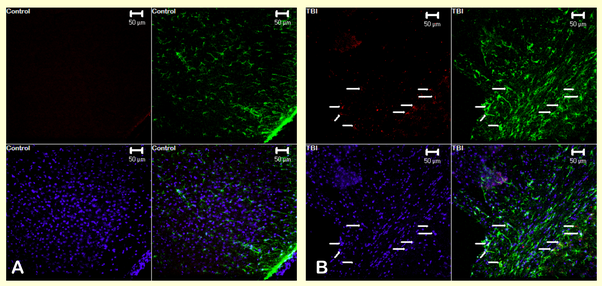

Figure2 : GFAP⁺ and Tau⁺ cell types in peri-lesional cortical areas in post-TBI (B) compared to control (A) brain sections. Each image is a composition of four images of red, green blue and composite channels separately and bottom right image is the superimposed image. Drastic increase in GFAP IR in the post-TBI section shows that the GFAP⁺ cell types are more present in the post TBI. Tau⁺ cells are little in the control (A) compared to the TBI (B). The merged image at the bottom right corner of each image shows and many Tau⁺ and GFAP⁺ colocalization (see the white arrows). Green: Rat Anti-GFAP antibody (1:100) developed using Alexa 488® and Red: mouse monoclonal anti-Tau antibody (1:100) and Alexa 594®; Blue: DAPI nuclear staining.

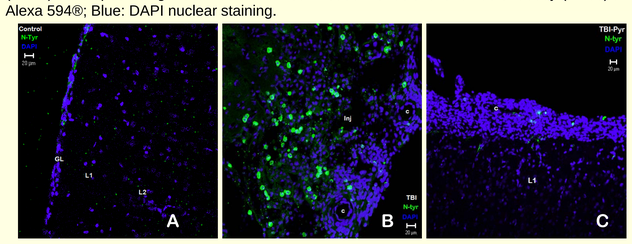

Figure 3: Comparison of nitrotyrosine (N-Tyr) IR in TBI cortical lesional areas (B) compared to uninjured iso-cortex (A) and Sod. Pyruvate (Pyr) treatment (C). L1 and L2 are iso-cortical pyramidal layers 1 and 2; GL: is ensheathing glial limitans (dense DAPI nuclear stained layer). Note that instead of GL, there is a large increase in cell density in the peri-lesional areas associated with blood capillaries (c). The amount of nitrotyrosine formation is evident even on the 7th day post injury. Note the drastic decrease of N-Tyr IR in Pyruvate treated brain section. Green: Mouse Anti Nitro-tyrosine (1:100) and Goat Anti-Mouse Secondary antibody coupled to Alexa 488 ® . Blue: DAPI Nuclear Staining.

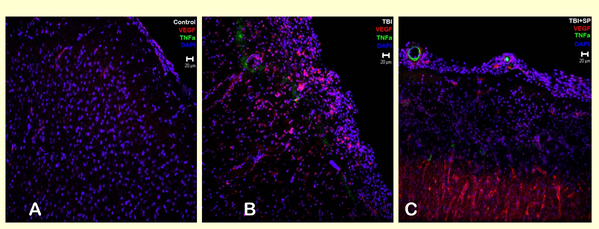

Figure 4: VEGF and TNF-α expression in the peri-lesional area of rat cortex is shown. The immunoreactivity is very less in control, but their expression is higher in TBI and intense in Sod. Pyruvate (SP) treated TBI. The VEGF expression (Red) pattern changes with treatment (in C compared to B) so that more expression around blood cortical vessels showing an increased vascular formation with treatment (C). The TNF α (Green) is much more intense in C compared to B. Rabbit Anti VEGF (1:1000): Red Alexa 594; Mouse TNF α (1:50): Green Alexa 488; DAPI-Blue. A, B, C-20x obj, D-40x oil obj. GL-Glial Limitans; C: Capillaries; bv- blood vessels; L1-Layer 1 neo-cortex

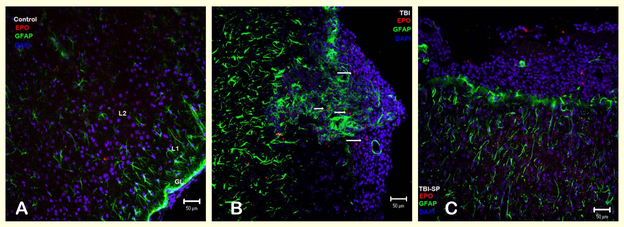

Figure 5: Comparative IR of Erythropoietin and GFAP in the superficial neocortical area with (B)without (A) TBI and post TBI treatment with Sod. Pyruvate (C). GFAP IR in green shown that the glial limitans in A (Control) is breached in B (TBI) & C (TBI+SP). EPO IR near the peri-lesional capillaries are shown by red spots on the tip of white arrows in B. Note the significant reduction in EPO IR in C suggesting a decrease in the EPO IR after SP treatment. Also, the GFAP IR is decreased in C (SP treated) compared to untreated (B) or shown in Figure 2. Rabbit Anti-EPO (1:50) and Goat anti-Mouse IgG coupled to Alexa 594® giving Red; Rat Anti-GFAP (1:100) and goat anti-rat IgG coupled to Alexa 488 ® giving green and DAPI nuclear staining giving blue fluorescence.

Conclusion

Potential Cytokine Markers for TBI

Cytokines	Increased (↑)or Decreased (↓)in TBI compared to Control	Significance
β-NGF	↑	Neuronal specific growth factor
CINC-3	↑	Pro-inflammatory: Neutrophil chemo-attractant (*4*)
FasLigand	↑	Pro-apoptotic: Attaches to Fas-FasR
GM-CSF	↓	Pro-inflammatory: Macrophage induction
IL-1β	↑	Pro-inflammatory: Lymphocyte mitogen
IL-1 R6	↓	Pro-inflammatory: CNS and vascular binds to 1L-1α (*5*)
IL-6	↑	Pro-inflammatory: vascular smooth muscle contraction; Anti-inflammatory: inhibits TNF-α
IL-10	↑	Anti-inflammatory: inhibits Th1 specific cytokine expressions and NF-κB activity
IL-13	↑	Pro-inflammatory allergic reactions: binds to IL-4
LIX	↓	Pro-inflammatory: LPS inducible CXC chemokine ligand5 (TNF-α induced)
PDGF-AA	↓	Mitogen/Anti-apoptotic : Homodimeric proteins binds to TK-receptor
Prolactin-R	↓	Growth Factor (*6*)
TNF-α	↓	Pro-inflammatory: multiple functions
VEGF	↓	Angiogenesis and Growth Factor
Nitotyrosine	↑	Indicator of formation of Peroxynitrite and ROS
EPO	↑	Indicator of angiogenesis

Future Directions

The potential cytokine markers described in the present study needs to be studied in the immediate lesional areas and compared against the global change as exemplified here with four markers so that they can be established and used as peripheral markers of extend of injury once they are established locally.

References

1. Sharma P et al., 2009. J Emerg Trauma Shock. 2(2): 67–72.
2. Manion ST et al., 2007. Pharmacol. Biochem. and Behavior, 86(3):559-565.
3. Ariyannur PS et al., 2010. J Comp. Neurol. 518:2952–2977
4. Takano K et al., 2001. Inflamm Res. 50(10):503-8.
5. Lovenberg TW et al., 1996. J Neuroimmunol. 70(2):113-22.
6. Ali S et al., 1998. J Biol Chem. 273(13):7709-16.

This research was supported by DARPA Grant W911NF111005 to PS

UNIFORMED SERVICES UNIVERSITY
of the Health Sciences